Title:

An agonist concentration biased allosteric modulator potentiates NMDA induced ion influx in neurons

Authors:

Blaise M. Costa[1,2,4*], Lina Cortés Kwapisz[1], Brittney Mehrkens[1], Douglas N. Bledsoe[1], Bryanna N. Vacca[1], Tullia V. Johnston[1], Anushri K. Wagner[2], Rehan Razzaq[2], Dhanasekaran Manickam[3], Bradley G. Klein[1&4]

[1]Center for One Health Research, Virginia Maryland College of Veterinary Medicine, Virginia Tech, [2]Edward Via Virginia College of Osteopathic Medicine (VCOM), [3]Syngene International, Bangalore, India, [4]School of Neuroscience, Virginia Tech, Blacksburg, VA 24060, USA.

Current address: DNB, Virginia Commonwealth University, Richmond, VA; BNV, University of North Carolina, Chapel Hill, NC.

***Corresponding author email address**: bcosta@vt.edu

Availability of data

The data that support the findings of this study are available from the corresponding author upon reasonable request. Some data may not be made available because of privacy or ethical restrictions

Abbreviations:

Ca2+: calcium ions

cDNA: complementary DNA

E18: Embryonic day-18

GluN: Glutamate receptor NMDA subtype

HEK293T: Human embryonic kidney 293 transfectable

MTS: 3-(4,5-dimethylthiazol-2-yl)-5-(3-carboxymethoxyphenyl)-2-(4-sulfophenyl)-2H-tetrazolium

Na+: Sodium ions

NMDA: N-methyl D aspartate

TEVC: Two Electrode voltage clamp

Abstract:

Background and purpose:

Precisely controlled synaptic glutamate concentration is essential for normal function of the N-methyl D-aspartate (NMDA) receptors expressed in the brain. Atypical fluctuations in synaptic glutamate homeostasis lead to aberrant NMDA receptor activity that results in pathogenesis of neurological and psychiatric disorders. Therefore, glutamate concentration dependent NMDA receptor modulators will be clinically useful agents with less on-target adverse effects.

Experimental approach:

Two electrode voltage clamp and patch clamp electrophysiology techniques were used for pharmacological characterization. Dynamic Ca2+ and Na+ imaging were performed using cultured rat brain neurons. MTS cell viability assay was used for to study neurotoxicity.

Key results:

Identified a compound (coded as CNS4) that potentiates NMDA receptor currents based on the glutamate concentration. This compound increases both glycine and glutamate potency, and exhibits no voltage dependent effect. Electrophysiology recordings confirmed agonist concentration dependent changes in peak and steady state currents. Dynamic Ca2+ and Na+ imaging assays using rat brain cortical, striatal and cerebellar neurons revealed CNS4 mediated region specific disproportionate influx of Na+ compared to Ca2+ in native NMDA receptors. Direct exposure of CNS4 unaltered the viability of cultured cortical or striatal neurons, neither augmented NMDA induced neuronal death.

Conclusion and implications:

CNS4 is novel in chemical structure, mechanism of action and agonist concentration biased modulatory effect. This compound or its future analogs will be useful for the treatment of brain disorders associated with hypoglutamatergic neurotransmission.

Bullet point summary:

What is already known?

- Dysfunction of tightly calibrated glutamate homeostasis leads to an aberrant glutamatergic neurotransmission that results in brain disorders.
- Preexisting NMDA receptors compounds do not switch their activity based on the agonist concentration.

What this study adds?

- Identified a novel lead compound that potentiates inhibits or inhibits NMDA receptors when based on the glutamate concentration.
- Disproportionately potentiates Ca2+ and Na+ influx into neurons.

Clinical significance

- This compound or its future analogs will be useful for the treatment of neuropsychiatric disorders that are associated with the dysfunction of synaptic glutamate homeostasis.

Introduction

Dysfunction of glutamate homeostasis in the brain is associated with the pathogenesis of psychiatric and neurological disorders in human beings (Volk, Chiu, Sharma & Huganir, 2015). Major glutamatergic neurotransmission occurs in the brain through N-methyl-D-aspartate (NMDA) subtype of inotropic glutamate receptors that are composed of two identical glycine binding GluN1 and two identical or different glutamate binding GluN2 polypeptide chains, referred as subunits, of which there are four different types GluN2A-D (Paoletti, Bellone & Zhou, 2013; Traynelis, 2010). Agonist mediated cascade of conformational changes occurring in the extracellular domains determine the distinct biophysical properties and downstream signaling mechanisms (Traynelis et al., 2010; Zhu & Gouaux, 2017; Zhu et al., 2016). Therefore, modulating NMDA receptor function based on the glutamate concentration would be an appropriate strategy to treat symptoms associated with the dysfunction of glutamate homeostasis.

It has been recently identified that positive and negative allosteric modulators share a common binding site (Perszyk et al., 2018). The physical energy required for the movement of extracellular domains, which is necessary to transform the receptor from activated to inactivated states, should be generated by binding of endogenous glutamate and glycine induced changes in entropy. Previous studies reported that the concentration of glutamate and glycine plays a crucial role in determining the desensitization of NMDA receptors (Benveniste, Mienville, Sernagor & Mayer, 1990; Nahum-Levy, Lipinski, Shavit & Benveniste, 2001). It was also evidenced by single channel recordings and mathematical modelling of channel open probability and mean open time that agonist concentration plays a crucial role in receptor desensitization (Kussius, Popescu & Popescu, 2010; Popescu, 2012). Whole cell NMDA receptor currents desensitize quicker and deeper when sub-saturating concentration of glycine is present. This phenomenon was referred to as glycine-dependent desensitization (Benveniste, Clements, Vyklicky & Mayer, 1990; Vyklicky, Benveniste & Mayer, 1990). However, precise modeling of glycine binding and

dissociation reactions onto a kinetic model of GluN1/2A receptors placed glutamate and glycine binding reactions on separate steps within the activation sequence that involves an avalanche of structural changes that results in channel opening (Iacobucci & Popescu, 2018). Similarly, at least two glutamate concentration dependent distinct desensitization states have been reported (Nahum-Levy, Lipinski, Shavit & Benveniste, 2001; Popescu, 2012). One results from weakening of glutamate affinity immediately after channel opening and the other form of desensitization occurs when channels enter into a long lived non-conducting state. Both glutamate and glycine binding and dissociation rate directly contribute to these different desensitized states (Nahum-Levy, Lipinski, Shavit & Benveniste, 2001).

Each different desensitized state should evolve from a unique conformational state of the receptor. Therefore, a family of distinct conformers should be sequentially formed and disappeared during the course of activation and deactivation process (Iacobucci & Popescu, 2018). Similarly, low and high agonist concentrations should, as they are capable of generating variable desensitization states, create distinct conformations of the receptor. We hypothesize that, if a compound can be interconverted to a positive or negative allosteric modulator by a methyl group (Perszyk et al., 2018), the binding pocket of this modulator should be a highly sensitive tipping point of the receptor. Conversely, geometry of such a binding pocket should get modified when the receptor adopts different conformational states when activated by high and low concentration of glutamate. Therefore, a suitable ligand should be able to discriminate the binding pockets formed by the low and high concentration of glutamate. This discrimination could lead to a potentiation or inhibition of the overall receptor current. In other words, instead of modifying a ligand to achieve different pharmacological effects, naturally occurring changes in the binding sites could be exploited for the benefit of desired modulatory effect by discovering appropriate ligands that can dissect GluN subunit function based on agonist concentration. In the present study, through our ongoing computational modeling and experimental screening efforts (Bledsoe

et al., 2017; Bledsoe, Vacca, Laube, Klein & Costa, 2019; Kane & Costa, 2015), we have identified and pharmacologically characterized a biased allosteric modulator (BAM) that potentiates NMDA receptor subunits based on the agonist concentration.

Materials and Methods

Synthesis of 4-fluoro-N-(2-(pyridin-3-yl)piperidine-1-carbonothioyl)benzamide (CNS004):

Anabasine, piperidinylpyridine alkaloid, based on a new thiourea was synthesized in two steps using thiocarbamoylation reaction. The starting 4-fluorobenzoyl isothiocyanate was synthesized in situ by heating 4-fluorobenzoyl chloride 1 with potassium thiocyanate in acetone. Further reaction of fluorobenzoyl isothiocyanate 2 with anabasine 3 in THF at room temperature yielded 4-fluoro-N-(2-(pyridin-3-yl)piperidine-1-carbonothioyl)benzamide (CNS004). The synthesized compound was confirmed by 1H-NMR & LCMS analysis and HPLC purity >99%. Detailed synthetic route and experimental procedures provided in the Extended Data Figure 1-1.

Two Electrode voltage clamp (TEVC) electrophysiology in xenopus oocytes: NMDA receptor constructs: cDNA encoding the NMDAR1a subunit (GluN1a) was obtained from Dr. Nakanishi (Kyoto, Japan). cDNA encoding the GluN2B (pci_sepGluN2B) was originally developed in Malinow lab (Kopec, Li, Wei, Boehm & Malinow, 2006), purchased from Addgene, Cambridge, MA. cDNA encoding the GluN2C and GluN2D were purchased from GenScript, New Jersey, USA. Mutated GluN1, 2A and 2B cDNA constructs capable of assembling as GluN1/2A/2B triheteromeric (1/2AB) receptors (Stroebel, Carvalho, Grand, Zhu & Paoletti, 2014) were obtained from Dr. Paoletti (Laboratoire de Neurobiologie, CNRS, France) These constructs have been previously tested for 1/2AB receptor activity of GluN1/2A receptor selective potentiators (Hackos et al., 2016). Plasmids were linearized with NotI (GluN1a wt) or AvrII (GluN2B), or BstB1 (GluN2C and GluN2D) and transcribed in vitro with T7 (GluN1/2A, GluN2B, GluN2C & GluN2D) RNA polymerase using the mMessae mMachine transcription kits (Invitrogen by Thermo Fisher

Scientific (Waltham, MA, USA) and SP6 (GluN1 mutants) RNA polymerase using the mMessage mMachine transcription kits (Ambion, Austin, TX, USA).

GluN subunit expression and electrophysiology in Xenopus oocytes: Stage IV frog oocytes were obtained from Xenopus-I, (Ann Arbor, MI, USA). NMDA receptor subunit cRNAs were suspended in nuclease free sterile water. GluN1A, GluN2B, GluN2C, GluN2D and GluN1/2A/2B cRNAs were mixed in a ratio of 1:1–3. 50 nL of the final cRNA mixture was microinjected (40–70 ng total) into the oocyte cytoplasm. Oocytes were incubated in ND-96 solution at 18°C prior to electrophysiological recordings (1–3 days).

Dose response curves: Electrophysiological responses were measured using a standard two-microelectrode voltage clamp [Warner Instruments (Hamden, Connecticut) model OC-725C] designed to provide fast clamp of large cells. The recording buffer contained 116 mM NaCl, 2 mM KCl, 0.3mM BaCl2, and 5 mM HEPES, pH 7.4. Response magnitude was determined in xenopus oocytes containing different NMDA receptor subunits (GluN1/2A, GluN1/2B, GluN1/2C, GluN1/2D and GluN1/2A/2B) by the steady plateau response elicited by bath application of different agonist concentration. 0.3uM, or 100μM or 300μM L-glutamate and 100 μM glycine were used to activate the receptors at a holding potential of −60 mV. Response amplitudes for functional NMDA receptors were generally between 0.1 and 2 μA. After obtaining a steady-state response to different agonist application, agonist plus CNS4 in different concentrations were applied (1 μM, 3μM, 10μM, 30μM and 100μM of CNS4 compound), using 8-channel perfusion system (Automate Scientific, Berkeley, CA), on the oocytes and the responses were digitized for quantification (Digidata 1550A and pClamp-10, Molecular Devices, Sunnyvale, CA). Dose- response relationships were fit to an appropriate curve fitting equation using GraphPad Prism-7, CA, USA. Non-linear regression was used to calculate IC50 or EC50 and percentage maximal inhibition. Statistical significance was determined at the alpha level $p < 0.05(*)$ using appropriate statistical methods as described in the relevant sections. Values given represent means (±) S.E.

Current-voltage (I-V) relationship experiments: I-V relationship was studied using xenopus oocytes expressing different NMDA receptor subunits (GluN1/2A, GluN1/2B, GluN1/2C and GluN1/2D) using 300nM L-glutamate + 100µM glycine or 100µM L-glutamate + 100µM glycine application at different holding potentials starting in -90mV up to + 30mV in 10mV intervals. After obtaining a steady-state response to different agonist applications, agonist plus 100µM CNS4 or agonist plus 40µM MgCl2 or agonist plus 100µM CNS4 or 40µM MgCl2 was applied. 40µM MgCl2 was chosen from the previously published experiments (Bledsoe, Vacca, Laube, Klein & Costa, 2019), since this was the IC50 (at -60mV) of GluN1/2A receptors. Data points were aligned by least square fit by third order polynomial equation, (Y=B0 + B1*X +B2*X^2 + B3*X^3). One-Way ANOVA with Tukey's multiple comparisons test, alpha level <0.05. Current values are obtained from the last one second of the 5 second application.

HEK-293T cells & whole cell patchclamp electrophysiology: Whole cell patch clamp electrophysiology studies were carried out in the HEK-293 cells, expressing recombinant NMDA receptors that lack native functional NMDA receptors (Matsuda, Fletcher, Kamiya & Yuzaki, 2003; Schuler, Mesic, Madry, Bartholomaus & Laube, 2008; Smothers & Woodward, 2007). Equal quantity of (1µg) cDNA for GluN1a, GluN2 (A or B or C or D) subunits will be co-transfected 24-48hrs before patch-clamp electrophysiology assay. Activation of NMDAR by ambient glutamate from the cell culture media was inhibited (to avoid excitotoxicity) by adding 50µM memantine into the culture media during transfection (Cousins, Papadakis, Rutter & Stephenson, 2008), cells will be carefully washed before performing experiments. Cells will be used for the electrophysiology experiments after 24 to 48hrs incubation in 37ºC with 5%CO_2. The whole cell patch clamp electrophysiology assay was performed using the semi-automated patch clamp equipment, Port-a-Patch (Nanion Technologies GmbH – Germany). The planar patch clamp chips used in Port-a-Patch are ideal for low noise recordings due to minimal capacitive charging and stray capacitance. They routinely give low and stable access resistance, which is important when studying ion

channels like NMDA receptors. Nanion NPC chips with 2-3.5 mOhms resistance were used for the HEK-293 cell recordings. Agonist concentrations used for this set of experiments are provided in the results section.

Primary Rat Brain Neuron Culture: E18-19 rat brain primary cortical & striatal neurons were cultured on poly-d-lysine coated 96 well plates for 14 days *in vitro* (DIV14) before using for the experiments. Primary rat brain cell culture was done as previously published (Peng et al., 2008) (Costa, Yao, Yang & Buch, 2013). Briefly, each well of 96 well plate was loaded with 50,000 cells and grown in neurobasal media supplemented with B27, glutamax, penicillin streptomycin. 100µL of media was replaced with fresh media once in four days.

Dynamic calcium assay was carried out, using Fluo-8 no wash kit (abcam, ab112129), as per the manufacturer's instructions with minor modifications to fit with experimental necessities. On DIV14 removed all 200µL media and replaced it with 100µL of HBSS and 100µL of Fluo-8 dye loading solution. Incubated the plates in 37C for 30min and in room temperature for 30min. Plates were added with 100ul of volume of test chemicals immediately before running the calcium flux assay by monitoring the fluorescence intensity at ex/em = 490/525nm using synergy microplate reader, BioTek, VT. Costar 96 well clear bottom black side plates were read from the bottom ten times with 60sec interval between each read. Temperature was set 37C and read speed was 100mSec. Similarly, manufacturer recommended protocol was followed for Na+ influx using cell permeable CoroNa green-AM (ThermoFisher, cat # C36676), and the plate was read at 492/516nm.

Data Analysis: Background (dye alone wells) OD values were subtracted from the treated wells for all time points. For the plots, background OD values were normalized to zero and the relative treated well relative fluorescence units values were plotted to present the dynamic calcium flux. One way ANOVA using Tuckey's multiple comparison test used to determine statistical significance of each treatment group with alpha level $p<0.05$.

MTS Assay: DIV14 neurons were treated with NMDA or other chemicals (as mentioned in the results section) overnight before performing cell viability assay using calorimetric MTS assay kit (abcam, ab197010). 100µL of 200µL of culture media, in which neurons were growing, was replaced with the treatment solution. 96-well plates were read at 490nm using microplate reader. OD values represent the relative amount of formazan product formed from metabolically active cells. Thus, higher OD values represent better viability. Statistical significance was determined by one way ANOVA Tuckey's multiple comparison test used to determine statistical significance of each treatment group with alpha level $p<0.05$.

Results

1. CNS4 potentiates NMDA receptor current in agonist concentration dependent manner

Synthetic route and chemical structure of CNS004 (referred as CNS4 in the text) has been provided in Figure 1A. CNS4 potentiates agonist induced NMDA receptor currents in glutamate concentration dependent manner (Figure.1B-J). Results from TEVC electrophysiology assay reveal that CNS4 potentiated 0.3µM glutamate evoked whole-cell recombinant GluN1/2C currents up to 5 fold and GluN1/2D up to 8 fold (Figure.1C). Interestingly, CNS4 had almost no effect (< 20% of potentiation) on GluN1/2C & 1/2D receptors when higher concentration (100 & 300uM) of glutamate was used to activate the receptor (Figure.1C). A pair of CNS4 dose response traces display the potentiation of 0.3µM glutamate current responses in GluN1/2C (Figure1.I) and 1/2D (Figure1.J) receptors. On the other hand, CNS4 potentiated GluN1/2A currents and elicited no effect on GluN1/2B receptors in the presence of 100µM glutamate (A-B). When receptors were activated by 0.3µM glutamate concentrations, CNS4 potentiated GluN1/2B and had negligible effect on GluN1/2A. Since GluN2A and GluN2B subunits are canonical representatives of NMDA receptors, the combination of these subunits containing tri-heteromeric GluN1/2AB receptors were studied. Also, recent studies identified GluN1/2AB receptors as predominant NMDA receptor subtypes expressed throughout the hippocampus and cortex (Al-Hallaq, Conrads, Veenstra &

Wenthold, 2007; Hansen, Ogden, Yuan & Traynelis, 2014; Luo, Wang, Yasuda, Dunah & Wolfe, 1997; Rauner & Kohr, 2011; Sheng, Cummings, Roldan, Jan & Jan, 1994; Tovar, McGinley & Westbrook, 2013). In the 1/2AB receptors, similar to the activity on GluN1/2B, CNS4 potentiated 0.3μM glutamate induced currents and minimally affected 100μM and 300μM glutamate evoked currents. Figure.1C summarizes the EC50 values of each subtype of NMDA receptor. Note: In order to confirm the expression of GluN1/2AB receptors and its pharmacological effect, we have performed a control experiment with a known GluN1/2B selective compound, ifenprodil. Since GluN1/2AB receptors contain both 2A and 2B be subunit, it was hypothesized that ifenprodil should give an intermediate EC_{50} on GluN1/2AB receptor compared to GluN1/2A and 1/2B receptors. IC_{50} values (1/2A:202.06 ±25.09, 1/2B: 4.66±1.33, 1/2AB, 20.30±9.05uM) obtained from the ifenprodil and dose response curves provided in the Extended Data Figure 1-2.

2. CNS4 alters agonist potency & efficacy in subtype specific manner

Potentiation of NMDA receptor currents could occur due to various reasons including increased agonist potency, slower desensitization, increased mean open time or channel open probability (Traynelis, 2010). In order to identify the changes in agonist potency, glycine and glutamate dose response curves were performed in the presence of 30μM CNS4. Results from these assays revealed that CNS4 significantly increased glycine potency in GluN1/2B and 1/2AB receptors and reduced it in 1/2A receptors (Figure 2). Conversely, there was an increase in glutamate potency in GluN1/2A & 1/2AB receptors but GluN1/2B glutamate potency was not increased (Figure 2A-F). These findings revealed that at least one of the reasons for CNS4 induced potentiation of NMDA receptors currents could be associated with increase in either or both agonist potency. Further, these findings indicate that minor inhibitions observed with current responses (Figure 1B) were not due to the competitive antagonistic effect of CNS4 at glutamate or glycine binding site.

In order to understand whether CNS4 alters the efficacy of glycine or glutamate we have studied CNS4 with either one of the two agonists (glycine and glutamate). For this assay, 100μM agonist

was used to maximally activate the receptors, and then one of the co-agonists, or one of the co-agonists and CNS4 was applied. This should reveal the modulatory effect of CNS4 in the absence of either of the co-agonists on the receptors that were pre-occupied by both agonists when CNS4 approached the receptor. Results from this assay revealed that CNS4 reduced glutamate alone induced currents in GluN1/2A and 1/2AB receptors (Figure 3A-F). However, surprisingly, CNS4 significantly increased glutamate alone induced currents in GluN1/2B receptors (Figure 3E). If this increase in current response is due to glycine site partial agonist-like activity of CNS4, it should have increased the currents in GluN1/2A receptors as well in the absence of glycine. Instead, it significantly decreased the current response in GluN1/2A. Similar observation was made with the GluN1/2AB receptors. However, it was an interesting observation that in GluN1/2AB receptors glutamate alone could retain 70% of the full agonist induced currents (Figure 3F). It is noteworthy that CNS4 has no chemical structure similarity to glycine or glutamate. Further, theoretically glycine binding site in the GluN1 subunit remains identical in all NMDA receptor subtypes. These observations indicate that CNS4 differentially modulates glutamate efficacy, and distinguishes the closest NMDA receptor family members, Glun1/2A and 1/2B and their offspring 1/2AB.

3. Voltage independent and GluN2 subtype specific activity of CNS4

The current-voltage (I-V) relationship studies have been done to determine the voltage dependent effect of CNS4. 100µM glutamate and 100µM glycine were used as agonist to activate the NMDA receptors. Agonist induced whole cell I-V relationship was studied in 10mV intervals ranging from -90mv to +30mv. The recording buffer contained 116 mM NaCl, 2 mM KCl, 0.3 mM $BaCl_2$, and 5 mM HEPES, pH 7.4. 100µM of CNS4 and/or 40µM $MgCl_2$ was used for the I-V experiments. 40µM $MgCl_2$ was chosen from the previously published experiments (Bledsoe, Vacca, Laube, Klein & Costa, 2019), as this concentration of $MgCl_2$ was found to be the IC50 (at -60mV) of GluN1/2A receptors.

CNS4 exhibited no voltage dependence in any of the four NMDA receptor subtypes studied, Figure 4A-D. CNS4 plus agonist induced currents closely followed the agonist alone current amplitudes throughout the voltage ramp studied. However, in GluN1/2C receptors CNS4 changed the reversal potential of permeant ions (barium and sodium) to less negative compared to the reversal potential of agonist alone experiments. When GluN1/2C receptors are potentiated, the inward currents live longer than the normal activation, and thus require more positive membrane potential to reverse the current direction. Further, even in the presence of Mg2+, CNS4 could still reduce the reversal potential in GluN1/2C. CNS4 had no significant effect on GluN1/2A or 1/2B receptor current reversal potential, Figure 4A-B. It is noteworthy that GluN1/2A and 1/2B are more sensitive to Mg2+ than GluN1/2C and 1/2D receptors (Kuner & Schoepfer, 1996; Monyer, Burnashev, Laurie, Sakmann & Seeburg, 1994). I-V experiments were also carried out with 0.3μM (low) glutamate, and these results are provided as Extended Data Figure 4-1. This set of experiments largely reproduced the results obtained from 100μM glutamate assay. However, notably in low glutamate concentration assay, CNS4 changed the reversal potential of permeant ions in both GluN1/2C and 1/2D receptors. This corroborates with the potentiation of GluN1/2C and 1/2D receptors (Figure 1I&J). CNS4 might facilitate the inward current of ions in GluN1/2C subunits at both low and high agonist concentrations. However it does so on GluN1/2D receptors only at low glutamate concentration. These results suggest that CNS4 affects the reversal potential of ions in NMDA receptor subtypes in the following order: GluN1/2C$_{(L,H)}$>1/2D$_{(L)}$>1/2B and 1/2A remains unaltered. L&H represent low (0.3uM) and high (100uM) glutamate respectively. Comparison of all four subunits I-V curves in the presence and absence of Mg2+ has been made and provided in the Extended Data Figure 4-2 (0.3uM glu) & Figure 4-3 (100μM glu). At no voltage step current responses were significantly different in the presence and absence of CNS4. This revealed that CNS4 activity is voltage independent, however reversal potential exhibits some degree of subunit selectivity.

4. Agonist concentration dependent effect of CNS4 in mammalian cells

It was previously reported that ion channel drug screening results obtained from xenopus oocytes were comparable with mammalian expression system (Dingledine, Roth & King, 1987; Kleckner & Dingledine, 1989; Kushner, Lerma, Zukin & Bennett, 1988). Therefore, to demonstrate the glutamate concentration dependent activity of CNS4 on NMDA receptors expressed in the mammalian cells where intracellular scaffolding proteins that are essential for formation of functional receptors could be different from the ones expressed in xenopus oocytes, we have carried out patch-clamp electrophysiology assay using HEK293T cells transfected with GluN1/2A or 1/2AB receptor subunit constructs. To study the agonist concentration dependent effect of CNS4, NMDA receptors were activated by low (0.3uM) or high (100uM) glutamate in the presence of 100µM glycine. CNS4 activity was studied in three different conditions: (**1**) CNS4 co-application with agonist, (**2**) agonist pre-application and (**3**) CNS4 pre-application. These conditions would reveal the effect of CNS4 on the NMDA receptors exist in unbound (apo) state and received equal opportunity to bind with CNS4 and/or agonists as they preferred (**1**), receptors existing in agonist pre-bound conformation when CNS4 approach the receptor (**2**), and in CNS4 pre-application condition, it receives preference to bind with the apo state receptors (**3**). Results obtained from these three sets of experiments are presented in Figure 5-7. Analysis of the maximum inducible currents obtained from CNS4 and agonist co-application experiments revealed that CNS4 potentiated 0.3µM glutamate induced GluN1/2A peak currents and inhibited 100µM induced currents (Figure. 5). In GluN1/2AB receptors, CNS4 did not potentiate 0.3µM glutamate induced currents, instead inhibited both 0.3µM and 100µM glutamate induced currents Figure.5. Desensitization and deactivation time constant tau (Ƭ) was calculated using exponential weighted fit component of clampfit 10.7 (pClamp) software. This analysis revealed that CNS4 did not alter the desensitization in GluN1/2A or 1/2AB receptors; however GluN1/2A deactivation time course was significantly increased (Ag, 710.9 ± 98.27ms, n=9 vs Ag+CNS4, 1067 ± 104.3ms, n=19, $p<0.05$, unpaired t-test) after CNS4 co-application. This reveals a slower dissociation of agonists from the GluN1/2A receptor. Results provided in Extended Data Figure 5-1.

In the agonist pre-application approach, we have analyzed the steady state currents before and after the CNS4 application (Figure 6). Results from this set of experiments show that CNS4 potentiated 0.3μM glutamate induced steady state current but it had no significant activity on 100μM glutamate induced steady state currents in GluN1/2A receptors. Conversely, in the GluN1/2AB receptors CNS4 inhibited 0.3μM glutamate induced steady state current, and minimally potentiated 100μM glutamate induced steady state current in GluN1/2AB receptors. The current amplitudes at the end of four second agonist or agonist plus CNS4 application was used for the analysis. In CNS4 pre-application experiments, interestingly, CNS4 potentiated 0.3μM but not 100μM glutamate induced peak currents in GluN1/2A receptors. Conversely, in GluN1/2AB receptors CNS4 inhibited the current evoked by both of these glutamate concentrations (Figure 7).

Agonist concentration and potentiation pairs, observed in patch clamp electrophysiology assays, do not necessarily match with the equivalent of that observed in the TEVC electrophysiology results. This could be because of the differences in expression system, state of the receptors when CNS4 molecules approach them, and solution application speed as previously reported (Gibb et al., 2018; Perszyk et al., 2018; Perszyk et al., 2020; Rosenmund, Stern-Bach & Stevens, 1998). Nonetheless, results from these sets of experiments reveal that CNS4 modulates the NMDA receptor currents based on the concentration of agonists, and this modulation is subunit dependent. Remarkably, three out of four subunits in GluN1/2AB and 1/2A are essentially identical. Thus GluN1/2AB is the closest family member of predominantly expressing GluN1/2A subtype of NMDA receptor, and CNS4 differentiates the function of these subunits in agonist concentration dependent manner.

A transient and completely reversible peak was observed while CNS4 alone (in the external solution) was pre-applied (Figure 7). This unexplained peak appeared only when 100μM glutamate was present in one of the lines of the perfusion system. Therefore, we have

hypothesized that this is an artifact or due to the seepage of agonist solution into the tip of CNS4 alone solution dispensing line. However, this peak was reproducibly smaller with GluN1/2A receptor compared to 1/2AB receptors (Figure 7). Indeed, this peak was as strong as the agonist induced peak in the 1/2AB receptors. In order to re-confirm that this peak appears only because of agonist seepage, we designed another experiment in such a way that will not have an agonist alone dispensing line in the perfusion system. In this experiment, the perfusion system had only three lines. (1) External (recording) solution, (2) 100µM CNS4 alone (3) 100µM CNS4 + 100µM agonist solution and other lines of the 8-channel perfusion system were physically blocked. We hypothesized that since there is no agonist alone line in this set of experiments, CNS4 alone pre-application should not generate a peak this time. In contrast to the expectation, the peak still appeared with both GluN2A and 1/2AB receptor recordings (Figure 8). CNS4 alone application induced a transient current in GluN1/2A receptors which was 17.24±1.6% of CNS4+ agonist induced current; and in GluN1/2AB receptors this peak was as high as 80.15±2.3% of maximal current response. However, these peaks were smaller than the ones appeared when agonist alone line was present (Figure 7). These findings indicate that CNS4 might act like a glutamate sensitizer on ambient or very low concentrations glutamate. Further, these findings corroborate with the increased glutamate potency in GluN1/2AB and GluN1/2A receptors in TEVC assay (Figure 2). Overall, this set of experiments suggested that CNS4 alters agonist efficacy based on the concentration of agonist, and might have a weak partial agonist like activity. 100µM CNS4 did not produce any measurable current response in untransfected HEK293T cells (Figure 8D). Therefore, CNS4 alone induced currents are NMDA receptor mediated.

5. CNS4 differentially potentiates Ca2+ and Na+ ion influx in cultured rat brain neurons

To further study the effect of CNS4 on native NMDA receptors, we have performed dynamic calcium and sodium imaging assays in cultured rat brain neurons using cell permeable Fluo-8 and CoroNa green AM dyes respectively. Cortical, striatal and cerebellar neurons were cultured for fourteen days in vitro (DIV-14) before studying the effect of CNS4 as mentioned in the methods

section. Results from fluo-8 calcium assay revealed that CNS4 (100µM) increased NMDA included calcium influx in agonist concentration dependent manner in cortex, striatum and cerebellum (Figure 9). 300µM NMDA increased the Ca2+ influx compared to the background control, and 50µM memantine reversed NMDA induced Ca2+ signal back to control level. These observations confirmed the expression of NMDA receptors in the cultured neurons and they respond to the known exogenous ligands. 100µM CNS4 in a vehicle (loading dye) with no NMDA produced no significant Ca2+ signal. This indicates CNS4 itself is not activating NMDA receptors or any other endogenous Ca2+ ion channels; also not indirectly increasing cytosolic Ca2+. CNS4 did not increase Ca2+ signal in the presence of 0.3, 1, 3µM NMDA (Figure 9.). However, 10µM or higher concentrations of NMDA significantly increased calcium signals compared to CNS4 alone treated cells. Interestingly, CNS4 plus 300µM NMDA treated cells produced 1.73 fold more Ca2+ signal compared to plain 300µM NMDA [mean relative fluorescence units (rfu) 15711 to 27274]. Similar comparison in striatal neurons revealed a robust 3.5 fold potentiation (mean rfu 7000 to 25038). However, CNS4 alone treatment significantly reduced Ca2+ signaling in the striatal neurons compared to the background control. This inhibition was reversed with the increasing concentrations of NMDA. In the 300µM NMDA treatment group, relatively less Ca2+ signal was observed in the striatal cells compared to cortex, although equal amounts of cells ($5x10^4$/well in 96-well plate) loaded in all 96well plates. This might be due to the expression of less calcium conducting GluN1/2D NMDA receptor (in addition to 1/2A & 1/2B) subtypes in striatal cells (Evans et al., 2012) (Kosinski et al., 1998). Alternatively, ambient glutamate present in the working solutions might have activated high glutamate sensitive subtypes of NMDA and/or calcium permeable non-NMDA glutamate receptors. Thus the addition of 300µM NMDA could not further increase the Ca2+ influx as much as in cortical neurons.

Results from the cerebellar neurons, where relatively less calcium permeable GluN1/2C subunit is predominately expressed (Evans et al., 2012), largely resembled with striatum pattern. However, Ca2+ signal in the cerebellum was relatively much smaller than that of striatum and

cortex (average maximum rfu, cerebellum 4964, striatum 25038 and cortex 27274). This is in agreement with the expression of relatively less calcium permeable GluN1/2C subunit in the cerebellum (Buller, Larson, Schneider, Beaton, Morrisett & Monaghan, 1994). Nonetheless, CNS4 plus 300µM NMDA potentiated Ca2+ signal compared to 300µM NMDA (rfu, 4964 vs 3351) in the cerebellar neurons.

Dynamic Na+ imaging assay carried out using intracellular Na+ binding dye (CoroNa green-AM) revealed that in cortical neurons NMDA significantly increased Na+ influx, with a mean difference of 3440rfu units compared to background (Figure.10). Remarkably, NMDA plus memantine further potentiated intracellular Na+ signal to the highest level (16057rfu) observed in the cortical neurons. CNS4 alone induced Na+ signal (15732rfu) was comparable to that of memantine plus NMDA. However, addition of 0.3µM NMDA with CNS4 reduced the sodium signal to the lowest level (-5221rfu). Negative numbers indicate mean rfu was lower than that of background. 1µM NMDA, in contrast to 0.3µM NMDA, potentiated Na+ signals (10481rfu). Further, 3µM NMDA produced significantly less Na+ signals (6568rfu) compared to 1µM NMDA. There was a stepwise increase in Na+ signal from 10 to 100µM NMDA. 300µM NMDA did not significantly increase the Na+ signals compared to 100µM NMDA. A similar pattern was observed with the striatal neurons with some exceptions. Here, 300µM NMDA did not increase the Na+ signal compared to the background. This might indicate that ambient glutamate induced background Na+ signal could not be further improved by 300µM NMDA. This corroborates with the results obtained in the striatal neurons Ca2+ assay, where NMDA induced signal, although significantly more than the background, was not as strong as that of cortical neurons (Figure 10). The difference in NMDA receptor subtype population or other factors might contribute to this difference. Furthermore, 0.3µM NMDA potentiated Na+ signal to the highest level in striatal neurons (25424rfu), as opposed to the inhibition observed in cortical neurons at this concentration.

In the cerebellar neurons, 300µM NMDA significantly increased Na+ signal (5578rfu) compared to background (0 rfu). Memantine+NMDA, CNS4 alone and 0.3µM NMDA plus CNS4 significantly increased Na+ signal in the cerebellar cells (Figure. 10), as they did with the striatum neurons. Notably, 0.3µM NMDA increased Na+ signal to the highest level in the cerebellar cells (25049rfu). This is consistent with the results obtained from the striatum at this NMDA concertation. With 1µM NMDA there was a significant reduction in sodium signal compared to 0.3µM (7254 vs 25049rfu). 3-300µM NMDA gradually increased Na+ signal in the cerebellum neurons. The highest level of sodium signal (25049rfu) observed at cerebellar cells was comparable with that of the other two brain regions (cortex, 16067rfu & striatum, 25424rfu) neurons studied. However, it is noteworthy that the highest Ca2+ signal, that was produced by 300µM NMDA plus CNS4, at cerebellar neurons (4964rfu) was about fivefold less than that of cortex (27274rfu) and striatum (25038rfu) (Figure 9.) These results reinforce that NMDA receptors expressed in the cerebellar neurons conduct less Ca2+ ions. Memantine induced increase in Na+ signal does not fit with the expected direction of Na+ movement through NMDA channel. However, when NMDA channel was blocked by memantine non-NMDA or other Na+ ion channels might have activated to maintain the sodium homeostasis across the membrane. However, if this is the case, there is no reason why CNS4 also increases the Na+ signal by itself, and with the lowest concentration (0.3 µM) of NMDA it could fluctuate the Na+ signals to the highest (striatal & cerebellar neurons) and lowest (cortical neurons) levels. These findings suggest that CNS4 mediated NMDA concentration dependent changes in Na+ signals observed might be associated with Na+ ion movement through the NMDA receptor channel.

6. CNS4 induced potentiation of ion influx in neurons does not increase toxicity

Calcium and sodium imaging assays revealed that CNS4 potentiates ion influx through native NMDA receptors expressed in cultured rat brain neurons. Based on this finding we hypothesized that CNS4 induced potentiation of NMDA receptors might lead to more neurotoxicity and further

reduction in the neuronal viability, compared to NMDA alone treatment. To study this, an MTS assay was performed using DIV-14 cortical and striatal neurons. Results from this assay revealed that overnight treatment with 100µM NMDA significantly reduced the viability of both cortical and striatal neurons compared to the vehicle treated group (Figure 11A&B). This reduction in viability was prevented by NMDA receptor uncompetitive antagonist memantine. In contrast to our hypothesis, none of the three concentrations (1,10&100µM) of CNS4 further reduced the viability of neurons compared to NMDA treatment. These results suggest that CNS4 induced NMDA receptor potentiation does not necessarily enhance pro-apoptotic signaling pathways. To confirm CNS4 by itself is not toxic to neurons we have performed a separate MTS assay on the DIV-14 cells treated with CNS4 alone and compared this treatment with memantine and vehicle treated cells. Results from this assay revealed that CNS4 does not reduce the viability of neurons compared the untreated cells in both cortical and striatal neurons (Figure 11C&D). Nonetheless, memantine treatment improved the viability of both cell types. This might suggest that memantine blocked excessive activation of NMDA receptors by ambient glutamate and glycine present in the neurobasal media, thus protecting neurons from excitotoxicity. Since CNS4 is not a channel blocker, nor an agonist, the viability of cells remained the same as vehicle controls. Overall, CNS4 is not neurotoxic by itself and it does not cause additional cell death when co-applied with 100µM NMDA.

Discussion

Levorotary glutamate is the primary excitatory neurotransmitter in the vertebrate central nervous system (Monaghan, Bridges & Cotman, 1989; Watkins, Davies, Evans, Francis & Jones, 1981). Pulsatile release and subsequent changes in glutamate concentration in the synapse are essential for maintaining normal brain physiology (Cherubini, Ben-Ari, Ito & Krnjevic, 1991; Clements, 1996; Clements, Lester, Tong, Jahr & Westbrook, 1992; Diamond & Jahr, 1997; Dzubay & Jahr, 1999; Moussawi, Riegel, Nair & Kalivas, 2011). Glutamate concentration exceeds

1mM in the synaptic cleft followed an action potential for less than 10mS, and rapidly returns to less than 20nM between two consecutive release events due to high affinity glutamate uptake by neurons and glial cells (Dzubay & Jahr, 1999). Further, glutamate seepage that occurs during the rapid rise and fall event causes a glutamate concentration gradient across the penumbra of the synapse, commonly known as extrasynaptic site. This concentration gradient at extrasynaptic sites varies over three orders of magnitude, ranging from 0.02 to 30μM as identified by electrophysiology and micro dialysis experiments (Chefer, Thompson, Zapata & Shippenberg, 2009; Herman & Jahr, 2007).

Glutamate receptor subtypes including NMDA receptor family co-evolved with these changes, that constantly occur at synapses, adopted distinct affinity for glutamate based on their de-novo expression at synaptic or extrasynaptic localizations (Hardingham & Bading, 2003). These adaptations, that results from the amino acid sequence differences in the agonist binding domain and other regions (Blaise, Sowdhamini, Rao & Pradhan, 2004), contribute for the distinct role of each subtype of NMDA receptors (Buller, Larson, Schneider, Beaton, Morrisett & Monaghan, 1994; Cull-Candy, Brickley & Farrant, 2001; Monyer, Burnashev, Laurie, Sakmann & Seeburg, 1994). Recent studies demonstrate that activation of extrasynaptic NMDA receptors signal pro-apoptotic (Aluclu, Arslan, Acar, Guzel, Bahceci & Yaldiz, 2008; Okamoto et al., 2009) events whereas synaptic NMDAR activation promotes pro-survival mechanisms (Hardingham & Bading, 2002; Hardingham & Bading, 2010; Paoletti, Bellone & Zhou, 2013). GluN1/2A subunits are reported to be expressed in the synapse and GluN1/2B and 1/2D at the extrasynaptic side (Hardingham & Bading, 2002; Hardingham & Bading, 2010). Therefore, disruption in glutamate hemostasis at synaptic or extrasynaptic compartment results in abnormal activation of these subtypes that results in neuropsychiatric disorders (Coyle, 2012; Paoletti, Bellone & Zhou, 2013; Traynelis et al., 2010). Therefore, drugs that modulate NMDA receptors based on surrounding glutamate concentration could be useful to treat conditions that require enhancing the activity of

a subpopulation of receptors that are hypo-activated either because of insufficient glutamate release or rapid uptake or both. In this study, we have identified a small molecule CNS4 that modulates NMDA receptor function based on subunit composition and agonist concentration.

Results from the TEVC assay indicated that CNS4 potentiated GluN1/2C and 1/2D receptors when activated with submaximal glutamate (Figure 1B). CNS4 potentiated GluN1/2A and 1/2B currents, although to a relatively lesser extent, when activated by 100µM glutamate (Figure 1B). Interestingly, in the presence of 300µM glutamate CNS4 had minimal or no activity on any of the five different subtype compositions studied (Figure 1B). Further analysis indicated CNS4 increased both glycine and glutamate potency in GluN1/2A, 1/2B and 1/2AB receptors, with an exception of 1/2B receptors (Figure 2). I-V experiments revealed that CNS4 activity is not voltage dependent in any of the four major subtypes. In the future, various concentrations of permeant ions will be studied to have a better understanding of the changes in reversal potentials observed with GluN1/2C receptors (Figure 4C). Patch clamp electrophysiology assay reinforced the agonist concentration dependent effects. CNS4 potentiated 0.3µM glutamate induced currents in GluN1/2A receptors but minimally inhibited GluN1/2AB receptors (Figure. 5). Agonist concentration and potentiation pairs observed in patch clamp electrophysiology assays do not necessarily match with the equivalent TEVC pair. This could be because of the differences in expression system, state of the receptors when CNS4 molecules approach them, and solution application speed as previously reported (Gibb et al., 2018; Perszyk et al., 2018; Perszyk et al., 2020; Rosenmund, Stern-Bach & Stevens, 1998). Collectively, these findings directed us to study the effect of CNS4, on Ca2+ and Na+ influx through the NMDA receptors expressed in cultured rat brain cortical, striatal and cerebellar neurons, by activating with various NMDA concentrations. While this assay would not reveal a GluN2 subunit selectivity, we anticipated this results would help demonstrate CNS4 induced ion influx through native NMDA receptors.

300µM NMDA induced Ca2+ ion influx was significantly higher in the presence of 100µM CNS4 in neurons of cortex, striatum and cerebellum (Figure 9). However, CNS4 alone significantly reduced the ion influx in the striatum compared to the background signal. Similar observation was made at the cerebellum as well but not in the cortical cells. This could happen from CNS4 blocking NMDA receptors that are previously activated by the ambient glutamate. This would lead to a question why no such reduction was noticed in the cortical neurons? Maybe due to the different subtypes of NMDA receptor population expressed in the cortex than in striatum and cerebellum (Buller, Larson, Schneider, Beaton, Morrisett & Monaghan, 1994). GluN1/2AB are found to be predominantly expressed in the cortical neurons. In the striatum, in addition to GluN1/2A and GluN1/2B receptors, GluN1/2D also expressed (Kosinski et al., 1998). It is possible that ambient glutamate might preferentially activate GluN1/2D receptors since this subtype of NMDA receptors have about three to six fold higher affinity for glutamate compared to GluN1/2A or 1/2B receptors (Erreger et al., 2007). This notion would also fit with the reduction in Ca2+ signals observed with CNS4 alone in the cerebellar neurons where GluN1/2C receptors are predominantly expressed. GluN1/2C receptors also have higher glutamate affinity compared to the canonical subunits of NMDA receptors. Thus, we propose CNS4 could have blocked the ambient glutamate induced activation of GluN1/2C & 1/2D receptors expressed in the cerebellar and striatal neurons.

Interestingly, memantine significantly increased intracellular Na+ signal in all three different populations of neurons, in contrast to the channel blockade mediated reduction that was anticipated (Figure 10). This could have happened due to the activity of various families of sodium channels expressed in the neurons (no Na^+ channel blocker was used in the assay). However, these Na+ channel activities should have been nullified by the background correction. Therefore, this observation might indicate either Na+ influx through NMDA channel was not blocked by memantine or memantine might directly or indirectly increased the Na+ influx into the neurons in order to maintain the electrolyte homeostasis across the membrane. Further, CNS4 alone also

increased Na+ signal in neurons from all three brain regions (Figure 10). However, addition of as little as 0.3µM NMDA (note: NMDA is a weak agonist to NMDA receptor with about three fold less potency than glutamate (Garthwaite, 1985) created a turbulence in the Na+ signal. For example, in the cortical neurons addition of 0.3µM NMDA with CNS4 produced the lowest level of Na+ signal which is diagonally opposite the highest level of Na+ signal observed with CNS4 alone. In contrast to this, 0.3µM NMDA produced the highest level of Na+ signal observed both in striatal and cerebellar neurons. Notably in these regions, 0.3µM NMDA plus CNS4 potentiated the CNS4 alone used signal. These findings direct us to consider that the changes in sodium signals observed with memantine or CNS4 alone could be associated with NMDA receptor channel activity and not completely due to non-NMDA channel activity. Notably, Na+ signal in cerebellar neurons was comparable with cortical and striatal neurons, whereas cerebellar calcium signal was about three fold less than that of cortex and striatal neurons (Figure 9&10). Overall, CNS4 evokes a distinct agonist concentration dependent Ca2+ and Na+ influx through the NMDA receptors.

CNS4 mediated increase in potency of lowest concentration of NMDA receptor agonist (NMDA) might explain the transient and completely reversible peak that was observed in the patch clamp assay when CNS4 alone was pre-applied on GluN1/2AB and 1/2A receptors (Figure 7). This peak might have appeared due to a rapid Na+ influx when there was little more than ambient concentration of glutamate was present around the cell. To recall, when 0.3µM glutamate was used as an agonist no such peak appeared (Figure 7). Maybe the amount of leftover (after washout) glutamate, which should be at least hundred fold less than the highest concentration (0.3uM) used in this experiment, present in the vicinity of the cell was insufficient to evoke currents to produce such a transient peak.

Excessive influx of ions through the NMDA receptor channel can lead to the excitotoxicity (Traynelis, 2010). Therefore, CNS4 induced excessive influx of ions could potentially lead to

reduction in neuronal viability. In contrast, there was no further increase in NMDA induced cell death when treated with 1 or 10 or 100µM CNS4, neither did CNS4 kill neurons by itself (Figure 11). Probably CNS4 induced potentiation was not activating pro-apoptotic pathways in neurons. However, CNS4 did not protect the neurons as memantine did. This is conceivable that memantine blocks NMDA channel but CNS4 does not. Therefore, an in vitro assay with hypo-glutamatergic condition would be more appropriate to study the beneficial effect of CNS4. We are planning to perform these assays in the near future. Overall, this biased allosteric modulator or its future analogs will be useful for the treatment of brain disorders that results from the dysfunction of synaptic glutamate homeostasis.

Acknowledgments: Authors thank Daniel Monaghan, University of Nebraska Medical Center for providing scientific inputs, and Pierre Paoletti, Institut de Biologie de Ecole Normale Supérieure, France for sharing $GluN1_{6A}$, $GluN2A_{r1}$ and $GluN2B_{r2}$ DNA constructs. This work was supported by American Heart Association Scientist Development Grant (16SDG27480023) funded to BMC, and partially supported by the Virginia Tech center for one health research grant funded to BMC and BGK.

Author contribution: Conceptualization (BMC), funding acquisition and progress reports (BMC & BGK), experiments (BMC, LCK, BM, DNB, BNV, TVJ, AKW), data analysis (BMC, LCK, DNB, BNV, RR), chemical synthesis (DM), project administration and manuscript writing (BMC).

Conflict of interest statement: Authors declare no competing financial interest.

References:

Al-Hallaq RA, Conrads TP, Veenstra TD, & Wenthold RJ (2007). NMDA di-heteromeric receptor populations and associated proteins in rat hippocampus. J Neurosci 27**:** 8334-8343.

Aluclu MU, Arslan S, Acar A, Guzel A, Bahceci S, & Yaldiz M (2008). Evaluation of effects of memantine on cerebral ischemia in rats. Neurosciences 13**:** 113-116.

Benveniste M, Clements J, Vyklicky L, Jr., & Mayer ML (1990). A kinetic analysis of the modulation of N-methyl-D-aspartic acid receptors by glycine in mouse cultured hippocampal neurones. J Physiol 428**:** 333-357.

Benveniste M, Mienville JM, Sernagor E, & Mayer ML (1990). Concentration-jump experiments with NMDA antagonists in mouse cultured hippocampal neurons. J Neurophysiol 63**:** 1373-1384.

Blaise MC, Sowdhamini R, Rao MR, & Pradhan N (2004). Evolutionary trace analysis of ionotropic glutamate receptor sequences and modeling the interactions of agonists with different NMDA receptor subunits. J Mol Model 10**:** 305-316.

Bledsoe D, Tamer C, Mesic I, Madry C, Klein BG, Laube B*, et al.* (2017). Positive Modulatory Interactions of NMDA Receptor GluN1/2B Ligand Binding Domains Attenuate Antagonists Activity. Front Pharmacol 8**:** 229.

Bledsoe D, Vacca B, Laube B, Klein BG, & Costa B (2019). Ligand binding domain interface: A tipping point for pharmacological agents binding with GluN1/2A subunit containing NMDA receptors. Eur J Pharmacol 844**:** 216-224.

Buller AL, Larson HC, Schneider BE, Beaton JA, Morrisett RA, & Monaghan DT (1994). The molecular basis of NMDA receptor subtypes: native receptor diversity is predicted by subunit composition. J Neurosci 14**:** 5471-5484.

Chefer VI, Thompson AC, Zapata A, & Shippenberg TS (2009). Overview of brain microdialysis. Curr Protoc Neurosci Chapter 7**:** Unit7 1.

Cherubini E, Ben-Ari Y, Ito S, & Krnjevic K (1991). Persistent pulsatile release of glutamate induced by N-methyl-D-aspartate in neonatal rat hippocampal neurones. J Physiol 436**:** 531-547.

Clements JD (1996). Transmitter timecourse in the synaptic cleft: its role in central synaptic function. Trends Neurosci 19**:** 163-171.

Clements JD, Lester RA, Tong G, Jahr CE, & Westbrook GL (1992). The time course of glutamate in the synaptic cleft. Science 258**:** 1498-1501.

Costa BM, Yao H, Yang L, & Buch S (2013). Role of Endoplasmic Reticulum (ER) Stress in Cocaine-Induced Microglial Cell Death. Journal of neuroimmune pharmacology : the official journal of the Society on NeuroImmune Pharmacology.

Cousins SL, Papadakis M, Rutter AR, & Stephenson FA (2008). Differential interaction of NMDA receptor subtypes with the post-synaptic density-95 family of membrane associated guanylate kinase proteins. J Neurochem 104**:** 903-913.

Coyle JT (2012). NMDA receptor and schizophrenia: a brief history. Schizophr Bull 38**:** 920-926.

Cull-Candy S, Brickley S, & Farrant M (2001). NMDA receptor subunits: diversity, development and disease. Curr Opin Neurobiol 11**:** 327-335.

Diamond JS, & Jahr CE (1997). Transporters buffer synaptically released glutamate on a submillisecond time scale. J Neurosci 17**:** 4672-4687.

Dingledine R, Roth AA, & King GL (1987). Synaptic control of pyramidal cell activation in the hippocampal slice preparation in the rat. Neuroscience 22**:** 553-561.

Dzubay JA, & Jahr CE (1999). The concentration of synaptically released glutamate outside of the climbing fiber-Purkinje cell synaptic cleft. J Neurosci 19**:** 5265-5274.

Erreger K, Geballe MT, Kristensen A, Chen PE, Hansen KB, Lee CJ*, et al.* (2007). Subunit-specific agonist activity at NR2A-, NR2B-, NR2C-, and NR2D-containing N-methyl-D-aspartate glutamate receptors. Mol Pharmacol 72**:** 907-920.

Evans RC, Morera-Herreras T, Cui Y, Du K, Sheehan T, Kotaleski JH*, et al.* (2012). The effects of NMDA subunit composition on calcium influx and spike timing-dependent plasticity in striatal medium spiny neurons. PLoS Comput Biol 8**:** e1002493.

Garthwaite J (1985). Cellular uptake disguises action of L-glutamate on N-methyl-D-aspartate receptors. With an appendix: diffusion of transported amino acids into brain slices. Br J Pharmacol 85**:** 297-307.

Gibb AJ, Ogden KK, McDaniel MJ, Vance KM, Kell SA, Butch C*, et al.* (2018). A structurally derived model of subunit-dependent NMDA receptor function. J Physiol 596**:** 4057-4089.

Hackos DH, Lupardus PJ, Grand T, Chen Y, Wang TM, Reynen P*, et al.* (2016). Positive Allosteric Modulators of GluN2A-Containing NMDARs with Distinct Modes of Action and Impacts on Circuit Function. Neuron 89**:** 983-999.

Hansen KB, Ogden KK, Yuan H, & Traynelis SF (2014). Distinct functional and pharmacological properties of Triheteromeric GluN1/GluN2A/GluN2B NMDA receptors. Neuron 81**:** 1084-1096.

Hardingham GE, & Bading H (2002). Coupling of extrasynaptic NMDA receptors to a CREB shut-off pathway is developmentally regulated. Biochimica et biophysica acta 1600**:** 148-153.

Hardingham GE, & Bading H (2003). The Yin and Yang of NMDA receptor signalling. Trends Neurosci 26**:** 81-89.

Hardingham GE, & Bading H (2010). Synaptic versus extrasynaptic NMDA receptor signalling: implications for neurodegenerative disorders. Nature reviews Neuroscience 11**:** 682-696.

Herman MA, & Jahr CE (2007). Extracellular glutamate concentration in hippocampal slice. J Neurosci 27**:** 9736-9741.

Iacobucci GJ, & Popescu GK (2018). Kinetic models for activation and modulation of NMDA receptor subtypes. Curr Opin Physiol 2**:** 114-122.

Kane LT, & Costa BM (2015). Identification of novel allosteric modulator binding sites in NMDA receptors: A molecular modeling study. J Mol Graph Model 61**:** 204-213.

Kleckner NW, & Dingledine R (1989). Selectivity of quinoxalines and kynurenines as antagonists of the glycine site on N-methyl-D-aspartate receptors. Mol Pharmacol 36**:** 430-436.

Kopec CD, Li B, Wei W, Boehm J, & Malinow R (2006). Glutamate receptor exocytosis and spine enlargement during chemically induced long-term potentiation. J Neurosci 26**:** 2000-2009.

Kosinski CM, Standaert DG, Counihan TJ, Scherzer CR, Kerner JA, Daggett LP*, et al.* (1998). Expression of N-methyl-D-aspartate receptor subunit mRNAs in the human brain: striatum and globus pallidus. J Comp Neurol 390**:** 63-74.

Kuner T, & Schoepfer R (1996). Multiple structural elements determine subunit specificity of Mg2+ block in NMDA receptor channels. J Neurosci 16**:** 3549-3558.

Kushner L, Lerma J, Zukin RS, & Bennett MV (1988). Coexpression of N-methyl-D-aspartate and phencyclidine receptors in Xenopus oocytes injected with rat brain mRNA. Proceedings of the National Academy of Sciences of the United States of America 85**:** 3250-3254.

Kussius CL, Popescu AM, & Popescu GK (2010). Agonist-specific gating of NMDA receptors. Channels (Austin) 4**:** 78-82.

Luo J, Wang Y, Yasuda RP, Dunah AW, & Wolfe BB (1997). The majority of N-methyl-D-aspartate receptor complexes in adult rat cerebral cortex contain at least three different subunits (NR1/NR2A/NR2B). Mol Pharmacol 51**:** 79-86.

Matsuda K, Fletcher M, Kamiya Y, & Yuzaki M (2003). Specific assembly with the NMDA receptor 3B subunit controls surface expression and calcium permeability of NMDA receptors. J Neurosci 23**:** 10064-10073.

Monaghan DT, Bridges RJ, & Cotman CW (1989). The excitatory amino acid receptors: their classes, pharmacology, and distinct properties in the function of the central nervous system. Annu Rev Pharmacol Toxicol 29**:** 365-402.

Monyer H, Burnashev N, Laurie DJ, Sakmann B, & Seeburg PH (1994). Developmental and regional expression in the rat brain and functional properties of four NMDA receptors. Neuron 12**:** 529-540.

Moussawi K, Riegel A, Nair S, & Kalivas PW (2011). Extracellular glutamate: functional compartments operate in different concentration ranges. Front Syst Neurosci 5**:** 94.

Nahum-Levy R, Lipinski D, Shavit S, & Benveniste M (2001). Desensitization of NMDA receptor channels is modulated by glutamate agonists. Biophys J 80**:** 2152-2166.

Okamoto S, Pouladi MA, Talantova M, Yao D, Xia P, Ehrnhoefer DE*, et al.* (2009). Balance between synaptic versus extrasynaptic NMDA receptor activity influences inclusions and neurotoxicity of mutant huntingtin. Nature medicine 15**:** 1407-1413.

Paoletti P, Bellone C, & Zhou Q (2013). NMDA receptor subunit diversity: impact on receptor properties, synaptic plasticity and disease. Nature Rev Neurosci 14**:** 383-400.

Peng F, Dhillon N, Callen S, Yao H, Bokhari S, Zhu X*, et al.* (2008). Platelet-derived growth factor protects neurons against gp120-mediated toxicity. Journal of neurovirology 14**:** 62-72.

Perszyk R, Katzman BM, Kusumoto H, Kell SA, Epplin MP, Tahirovic YA*, et al.* (2018). An NMDAR positive and negative allosteric modulator series share a binding site and are interconverted by methyl groups. Elife 7.

Perszyk RE, Swanger SA, Shelley C, Khatri A, Fernandez-Cuervo G, Epplin MP*, et al.* (2020). Biased modulators of NMDA receptors control channel opening and ion selectivity. Nat Chem Biol 16**:** 188-196.

Popescu GK (2012). Modes of glutamate receptor gating. J Physiol 590**:** 73-91.

Rauner C, & Kohr G (2011). Triheteromeric NR1/NR2A/NR2B receptors constitute the major N-methyl-D-aspartate receptor population in adult hippocampal synapses. The Journal of biological chemistry 286**:** 7558-7566.

Rosenmund C, Stern-Bach Y, & Stevens CF (1998). The tetrameric structure of a glutamate receptor channel. Science 280**:** 1596-1599.

Schuler T, Mesic I, Madry C, Bartholomaus I, & Laube B (2008). Formation of NR1/NR2 and NR1/NR3 heterodimers constitutes the initial step in N-methyl-D-aspartate receptor assembly. The Journal of biological chemistry 283**:** 37-46.

Sheng M, Cummings J, Roldan LA, Jan YN, & Jan LY (1994). Changing subunit composition of heteromeric NMDA receptors during development of rat cortex. Nature 368**:** 144-147.

Smothers CT, & Woodward JJ (2007). Pharmacological characterization of glycine-activated currents in HEK 293 cells expressing N-methyl-D-aspartate NR1 and NR3 subunits. The Journal of pharmacology and experimental therapeutics 322**:** 739-748.

Stroebel D, Carvalho S, Grand T, Zhu S, & Paoletti P (2014). Controlling NMDA receptor subunit composition using ectopic retention signals. J Neurosci 34**:** 16630-16636.

Tovar KR, McGinley MJ, & Westbrook GL (2013). Triheteromeric NMDA receptors at hippocampal synapses. J Neurosci 33**:** 9150-9160.

Traynelis SF (2010). Glutamate receptor ion channels: structure, regulation, and function. Pharmacol Rev 62**:** 405-496.

Traynelis SF, Wollmuth LP, McBain CJ, Menniti FS, Vance KM, Ogden KK*, et al.* (2010). Glutamate receptor ion channels: structure, regulation, and function. Pharmacol Rev 62**:** 405-496.

Volk L, Chiu SL, Sharma K, & Huganir RL (2015). Glutamate synapses in human cognitive disorders. Annu Rev Neurosci 38**:** 127-149.

Vyklicky L, Jr., Benveniste M, & Mayer ML (1990). Modulation of N-methyl-D-aspartic acid receptor desensitization by glycine in mouse cultured hippocampal neurones. J Physiol 428**:** 313-331.

Watkins JC, Davies J, Evans RH, Francis AA, & Jones AW (1981). Pharmacology of receptors for excitatory amino acids. Adv Biochem Psychopharmacol 27**:** 263-273.

Zhu S, & Gouaux E (2017). Structure and symmetry inform gating principles of ionotropic glutamate receptors. Neuropharmacology 112**:** 11-15.

Zhu S, Stein RA, Yoshioka C, Lee CH, Goehring A, McHaourab HS*, et al.* (2016). Mechanism of NMDA Receptor Inhibition and Activation. Cell 165**:** 704-714.

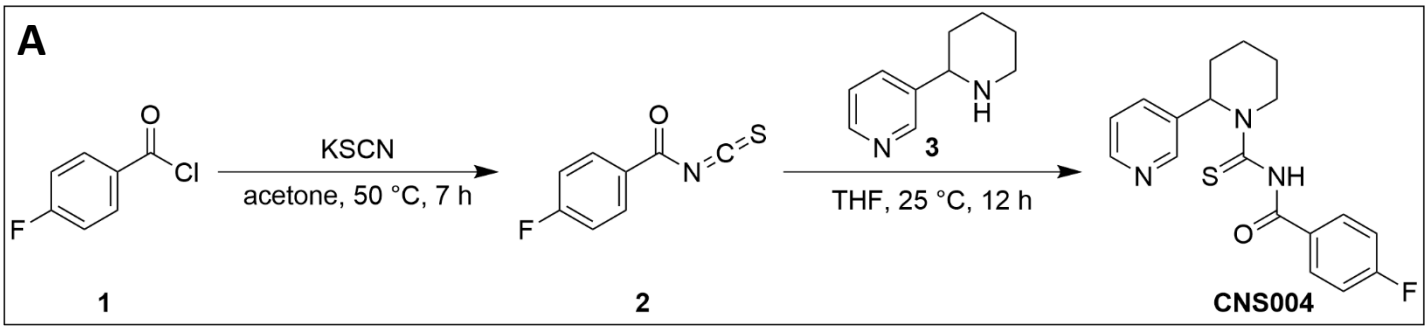

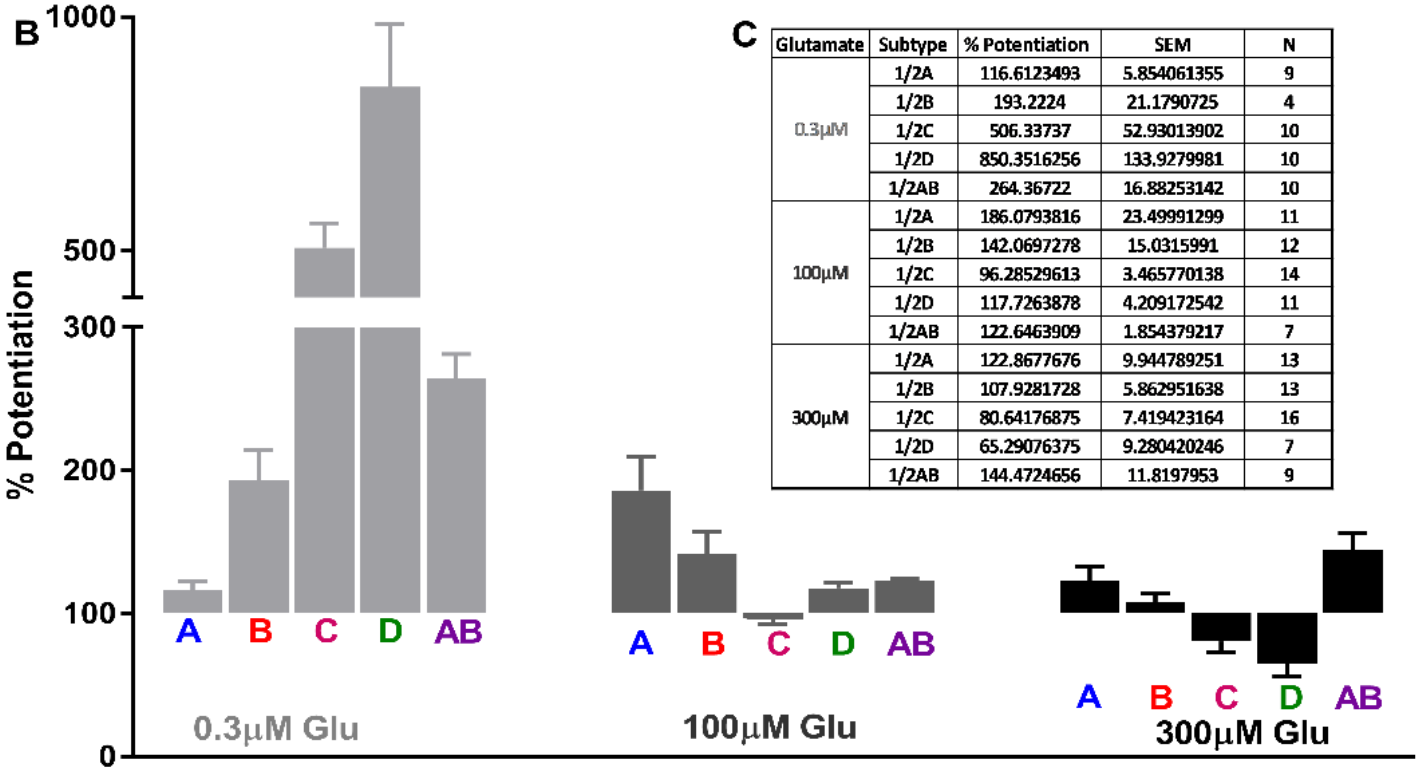

C

Glutamate	Subtype	% Potentiation	SEM	N
0.3μM	1/2A	116.6123493	5.854061355	9
	1/2B	193.2224	21.1790725	4
	1/2C	506.33737	52.93013902	10
	1/2D	850.3516256	133.9279981	10
	1/2AB	264.36722	16.88253142	10
100μM	1/2A	186.0793816	23.49991299	11
	1/2B	142.0697278	15.0315991	12
	1/2C	96.28529613	3.465770138	14
	1/2D	117.7263878	4.209172542	11
	1/2AB	122.6463909	1.854379217	7
300μM	1/2A	122.8677676	9.944789251	13
	1/2B	107.9281728	5.862951638	13
	1/2C	80.64176875	7.419423164	16
	1/2D	65.29076375	9.280420246	7
	1/2AB	144.4724656	11.8197953	9

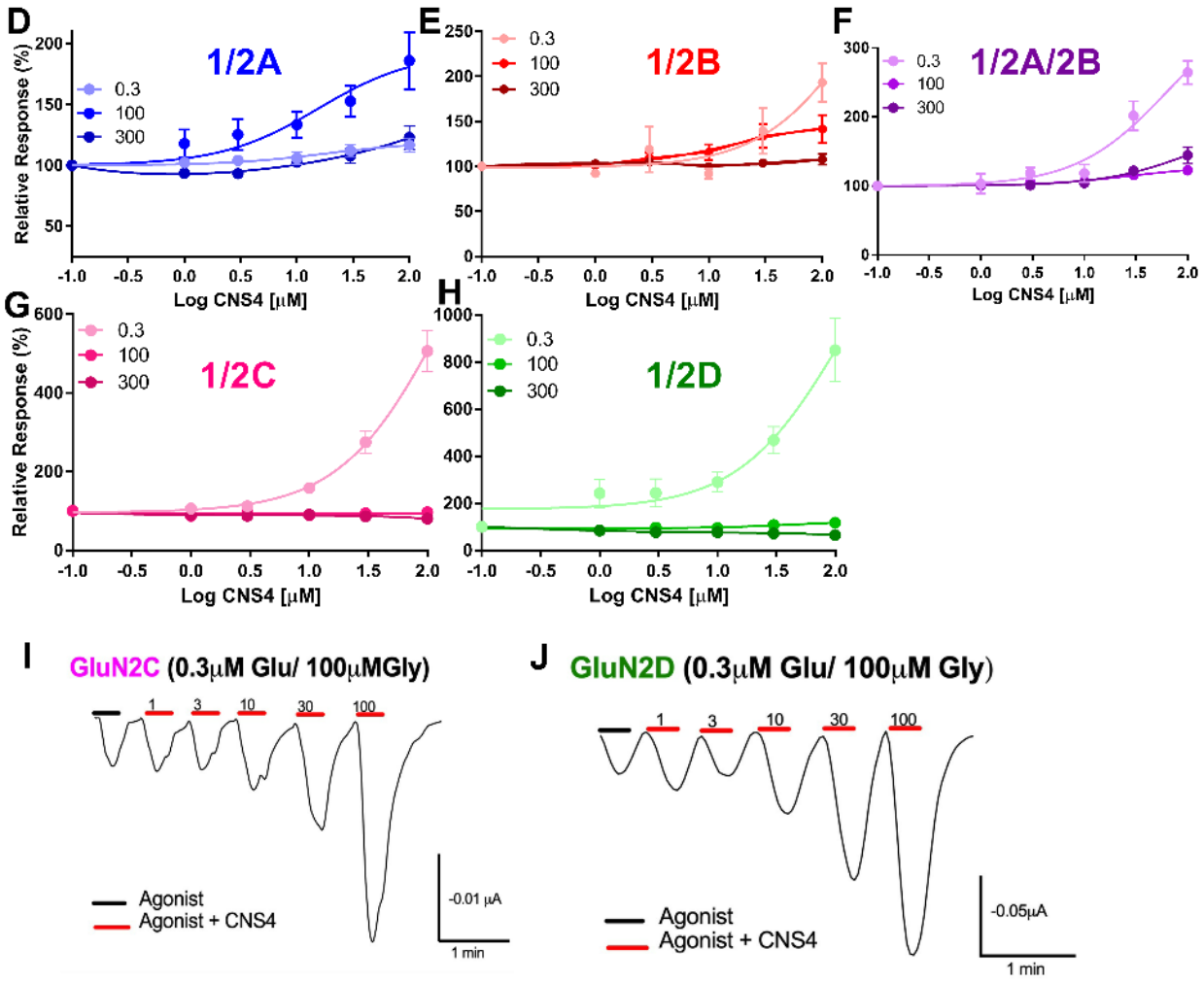

Figure-1. CNS4 potentiates NMDA receptor subtypes in agonist concentration dependent manner.

A. Synthetic route and chemical structure of CNS004 (referred as CNS4 in the text). More details on CNS4 synthesis provided in the methods section. Detailed synthetic route and experimental procedures provided in the Extended Data Figure 1-1. **B.** Effect of 100uM CNS4 on GluN1/2A, 1/2B, 1/2C, 1/2D receptors, and 1/2A and 2B subunit containing triheteromeric (AB) receptors with three (0.3, 100 & 300μM) different agonist concentrations. Receptor subtypes are labelled as, A(blue), B(red), C(maroon), D(green) & AB(purple) underneath respective histograms. **C**. (Table.1) shows the % potentiation. 100% represent the agonist induced maximal activation. Numbers more than hundred represent percentage potentiation. Numbers less than hundred represent relative percentage activation in the presence of 100μM. **D-H**, Dose response curves of NMDA receptor subunits as marked. Agonists labeled as light to dark colors corresponding to the increase in concentration. **I-J**, Representative traces GluN1/2C and 1/2D receptor potentiation with 0.3 μM glutamate. All agonist solutions contained 100μM glycine. Results confirming intermediate inhibitory effect of ifenprodil on GluN1/2AB receptors is provided in the extended data figure 1-2.

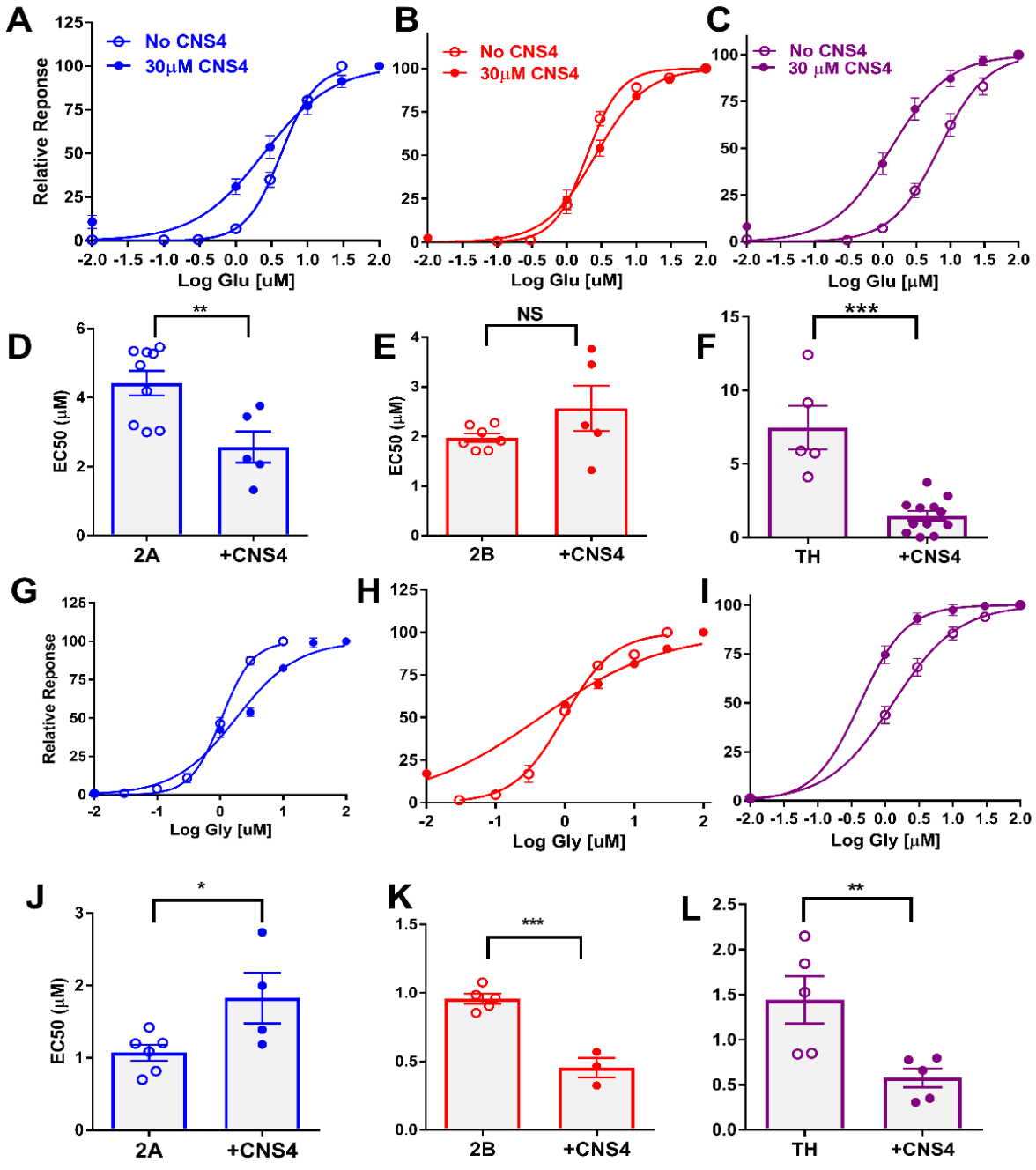

Figure-2. CNS4 increases agonist potency in NMDA receptor subtypes. Glutamate (**A-F**) and Glycine (**G-L**) dose response curve in the absence or presence of 30uM CNS4 on GluN1/2A, GluN1/2B and GluN1/2A/2B receptors. 100μM glutamate or glycine concentration was used for experiments. CNS4 reduced glutamate EC_{50} for GluN1/2A (4.42±0.36,n=9 vs 2.57±0.45uM,n=5 p<0.01), and GluN1/2AB (7.47±1.49,n=5 vs 1.48±0.33uM,n=12 p<0.001) receptors. EC_{50} of GluN1/2B receptors remained

unchanged (1.97±0.09, n=7 vs 2.57±0.45uM,n=5 p>0.05). Glycine EC_{50} increased 1/2A GluN1/2A (1.07±0.11,n=6 vs 1.83±0.35uM,n=4 p<0.05), and decreased in GluN1/2B (0.96±0.04,n=5 vs 0.45±0.07uM,n=3 p<0.001) and GluN1/2AB (1.44±0.26,n=5 vs 0.58±0.11uM,n=5 p<0.01) subunits. Values are average±SEM. Unpaired student's t-test, p<0.05. *p<0.05, **p<0.01 and ***p<0.001.

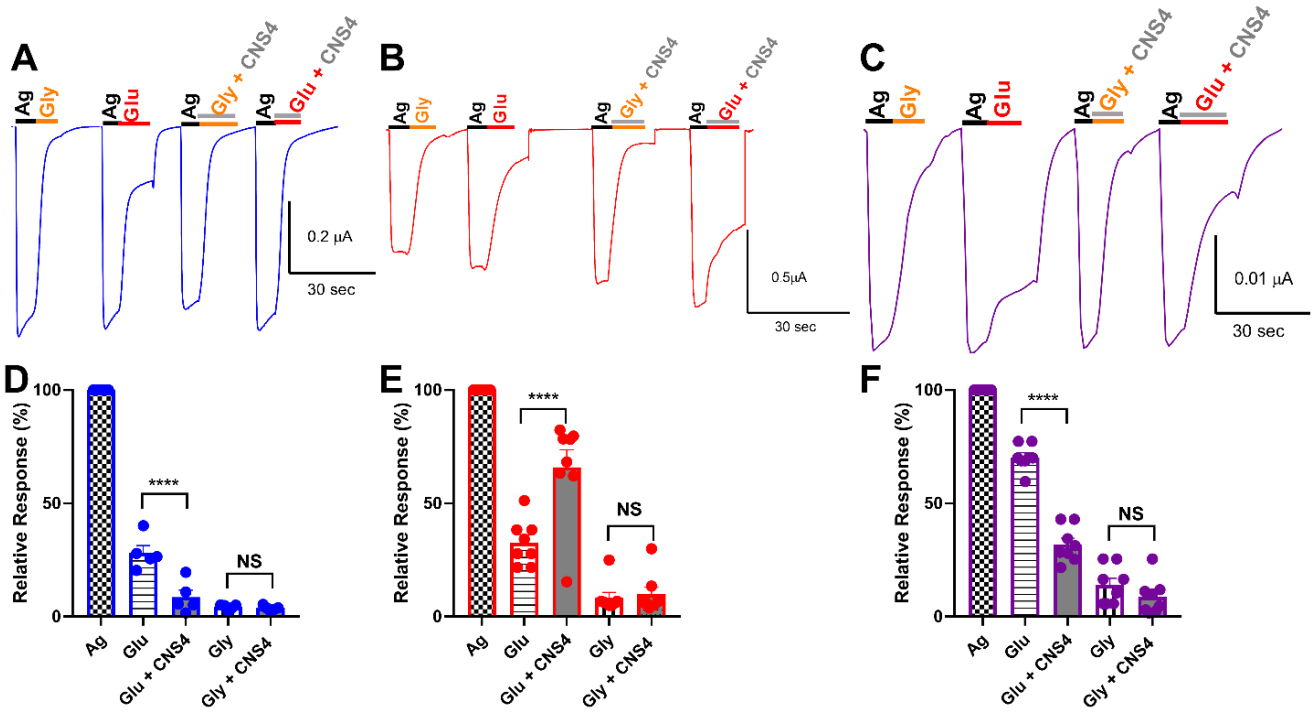

Figure-3. CNS4 increases glutamate efficacy in GluN1/2B receptors but reduces in GluN1/2A and 1/2AB receptors. Agonist contained 100uM glutamate + 100uM glycine (Ag, back bar) was used to maximally activate GluN1/2A (blue, **A**), 1/2B (red, **B**), and 1/2AB (purple, **C**) receptors to study the efficacy of glycine (orange bar), glutamate (red bar), glycine plus CNS4 (orange and gray bar), and glutamate plus CNS4 (red and gray bar) as labeled. 100uM CNS4 was used. In the absence of glycine, CNS4 reduced glutamate efficacy in GluN1/2A (28.06±3.27 vs 8.54±3.11%, n=5, p<0.0001) and 1/2AB (70.27±1.97 vs 31.85±2.76%, n=8) receptors. Conversely, CNS4 increased (32.62±3.52 vs 65.99±7.73%, n=8) glutamate in GluN1/2B receptors. In the absence of glutamate CNS4 did not alter the efficacy of glycine in any of the NMDA receptor subtypes studied. Values are average±SEM. One-way ANOVA with Sidak's multiple comparisons test, ****p<0.0001. NS= not significant, p>0.05.

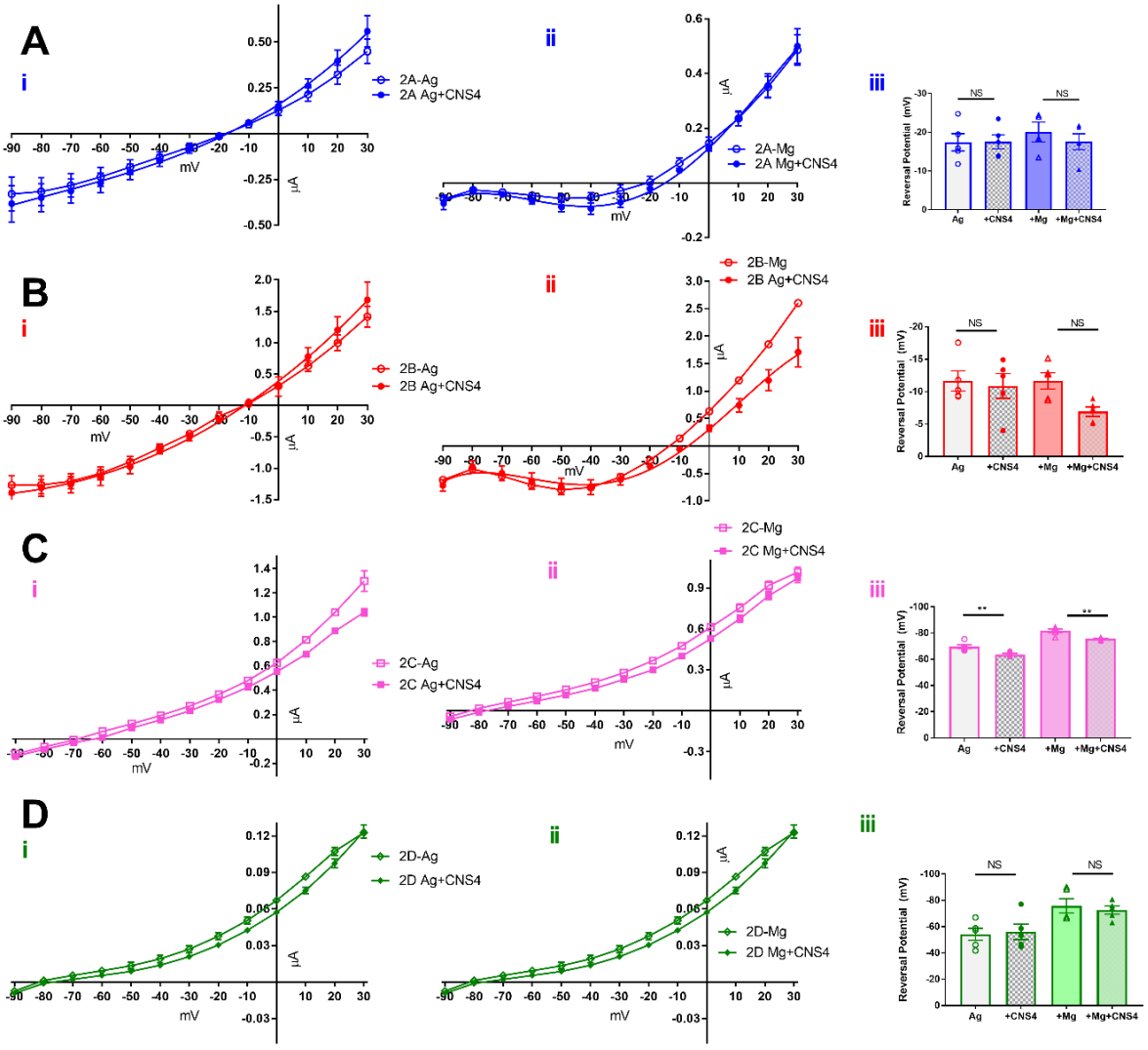

Figure-4. CNS4 activity on NMDA receptor subtypes is voltage independent. 100uM glycine and 100uM glutamate was used as agonist to activate the receptors. Agonist induced whole cell current-voltage (I-V) relationship was studied in 10mV intervals ranging from -90mv to +30mv. Data points were aligned by least square fit by third order polynomial equation, (Y=B0 + B1*X +B2*X^2 + B3*X^3), except for GluN1/2B that needed a fourth order polynomial equation. Reversal potential was obtained (from x-axis values when y=0.) for each individual recordings and then averaged. In GluN1/2C receptors, CNS4 altered the reversal potential in the absence (-69.55± 1.51 vs -63.64±0.80 mv, p<0.01, n=5) and presence (-81.75± 1.37 vs -75.53±0.59mv, p<0.01, n=5) of Mg2+. A similar reduction was not observed with GluN1/2D receptors (p>0.05, n=5). GluN1/2A and 1/2B receptor current reversal potentials remained unchanged by CNS4 when activated by 100uM glutamate (p>0.05, n=5 for 1/2A and 1/2B). Statistics, One-Way ANOVA with Tukey's multiple comparisons test, alpha level <0.05. Current values are obtained from the last one second of the 5 second application. Results from I-V experiments carried out with 0.3μM glutamate are

provided as Extended Data Figure 4-1. Comparison of all four subunits in the presence and absence of Mg^{2+} has been made and provided in the Extended Data Figure 4-2 (0.3uMglu) &4-3 (100µM glu).

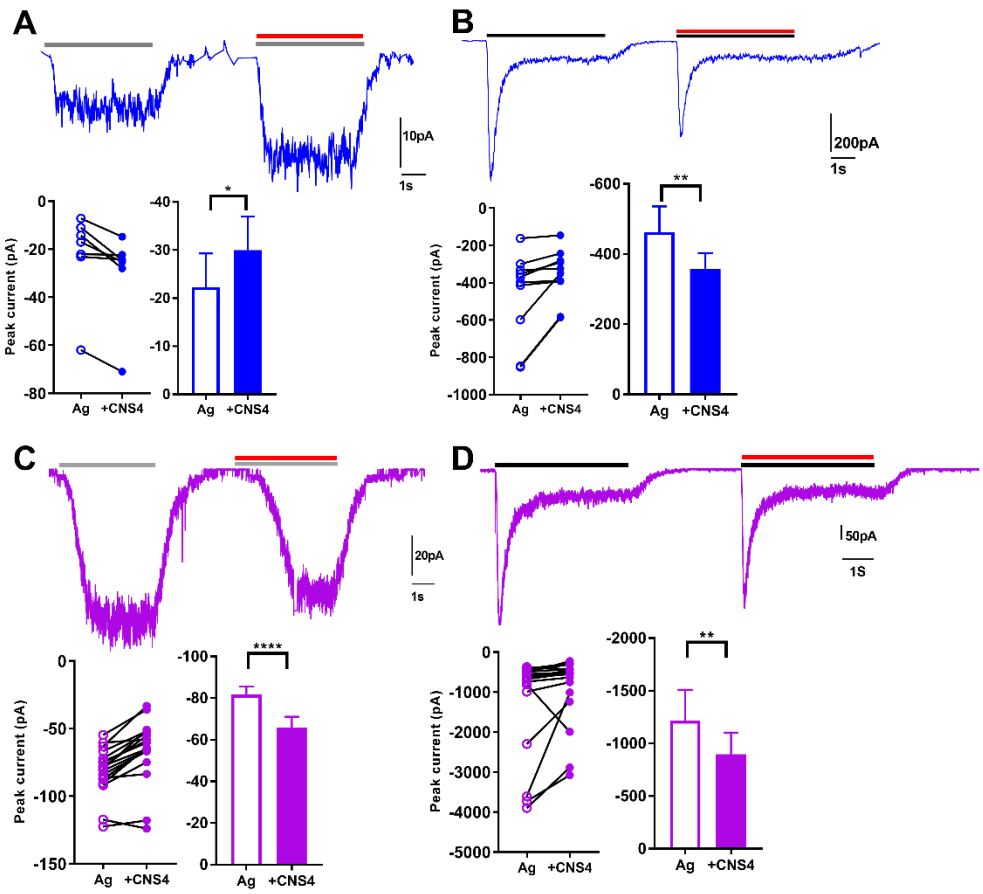

Figure 5. Co-application of agonist and CNS4 modulates GluN1/2A and 1/2AB currents in concentration dependent manner. Patch-clamp electrophysiology assays performed using HEK293T cells expressing GluN1/2A (blue) and GluN1/2AB (purple) receptors. Traces represent current responses evoked by 0.3 µM (**A&C**, gray bar) or 100 µM (**B&D**, back bar) glutamate and 100 µM glycine as agonist (Ag), and subsequent 100 µM CNS4 (red) co-application with agonist (+CNS4). Each pair of Ag and +CNS4 application events is shown in dot plots. Histograms show statistical significance. Wilcoxon matched-pairs signed rank test, *p<0.05, **p<0.01, ****p<0.0001. 0.3 µM Glu, 1/2A, n=7, 1/2AB, n=19 pairs. 100µM Glu, 1/2A, n=10, 1/2AB, n=18 pairs. Analysis of desensitization and deactivation time constant tau was calculated by exponential weighted fitting component of clampfit 10.7 (pClamp) software. These results are provided in Extended Data Figure 5-1.

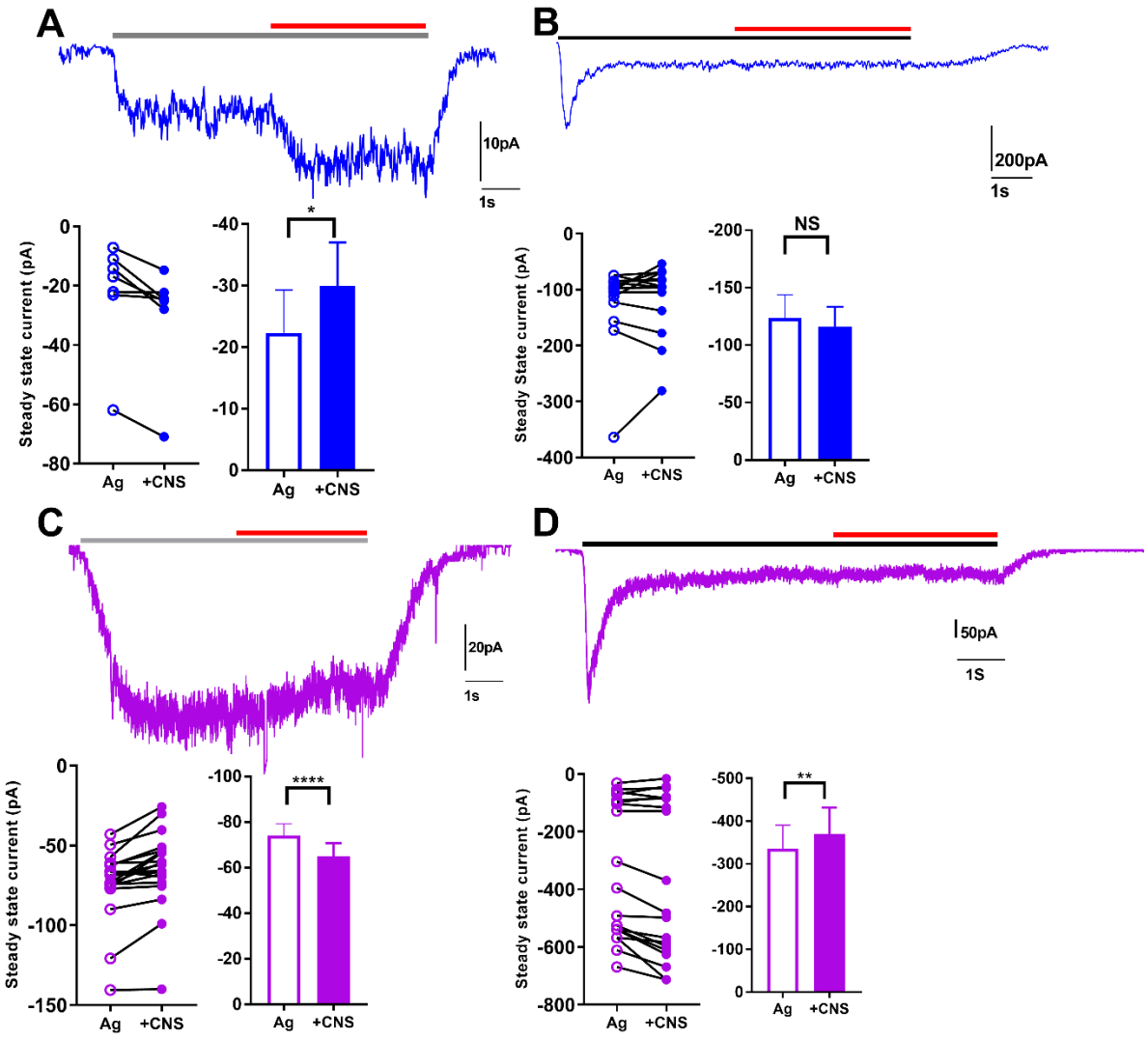

Figure 6. CNS4 modulates agonist induced steady-state currents in GluN1/2A and 1/2AB Receptors.

Whole cell patch-clamp electrophysiology assays performed using HEK293T cells expressing GluN1/2A (blue) and GluN1/2AB (purple) receptors. Traces represent current responses evoked by 0.3 µM (**A&C**, gray bar) or 100 µM (**B&D**, back bar) glutamate and 100 µM glycine as agonist (Ag), that was pre-applied before 100 µM CNS4 (red) co-application with agonist (+CNS4). Steady state current values obtained 4seconds after Ag application and 4s seconds after +CNS4 were used for the analysis. Each pair of Ag and +CNS4 application events is shown in dot plots. Histograms show statistical significance. Wilcoxon matched-pairs signed rank test, *p<0.05, **p<0.01, ****p<0.0001. 0.3 µM Glu, 1/2A, n=7, 1/2AB, n=19 pairs. 100µM Glu, 1/2A, n=14, 1/2AB, n=18 pairs. NS, not significant.

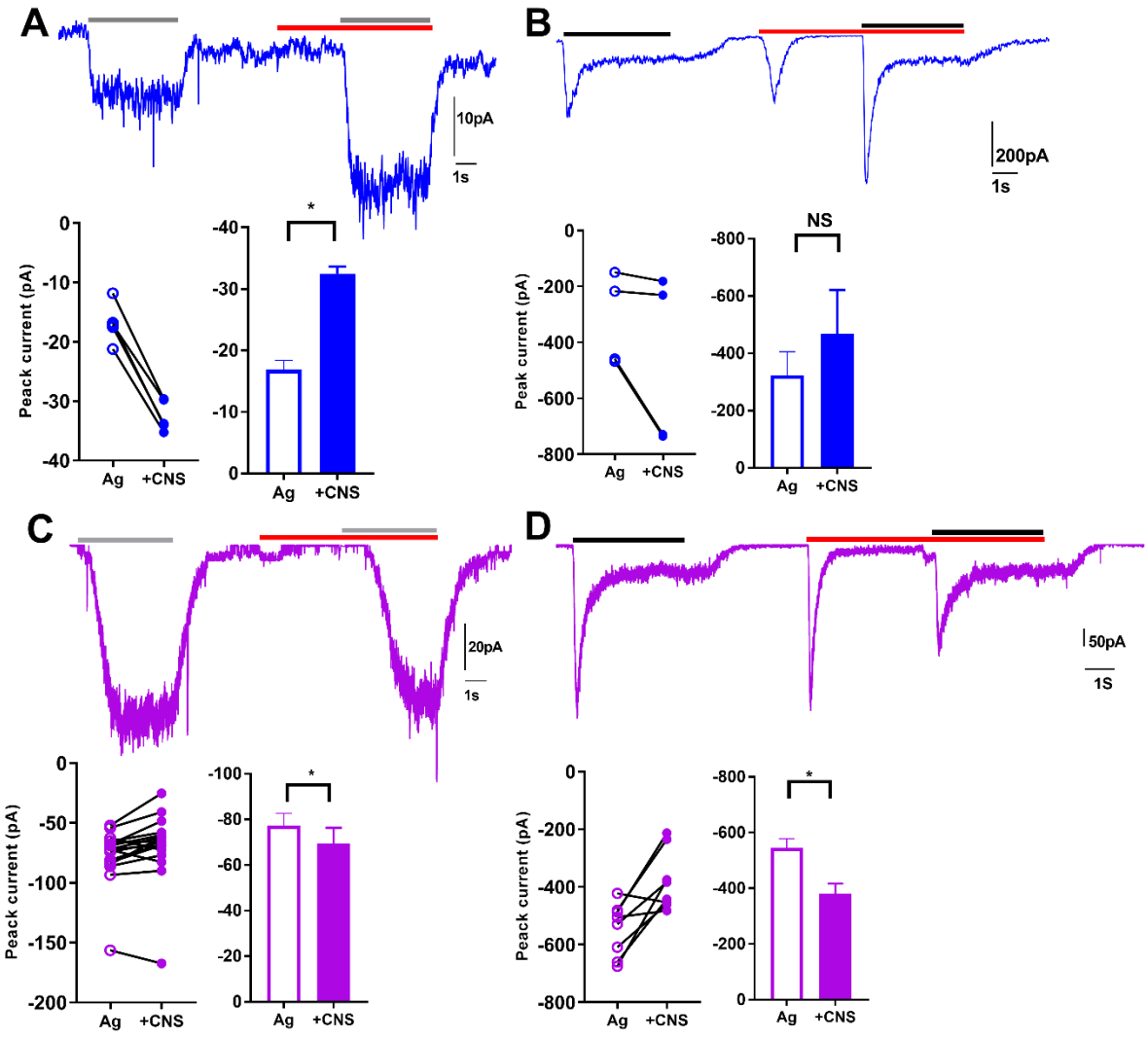

Figure 7. Pre-application of CNS4 modulates GluN1/2A receptor peak currents in concentration dependent manner. Whole cell patch-clamp electrophysiology assays performed using HEK293T cells expressing GluN1/2A (blue) and GluN1/2AB (purple) receptors. Traces represent current responses evoked by 0.3 µM (**A&C**, gray bar) or 100 µM (**B&D**, back bar) glutamate and 100 µM glycine as agonist (Ag). 100 µM CNS4 (red) was pre-applied before the co-application agonist (+CNS4). Peak current values of Ag application and +CNS4 were used for the analysis. Each pair of Ag and +CNS4 application events is shown in dot plots. Histograms show statistical significance. Wilcoxon matched-pairs signed rank test, *p<0.05, **p<0.01, ****p<0.0001. 0.3 µM Glu, 1/2A, n=5, 1/2AB, n=19pairs. 100µM Glu, 1/2A, n=4, 1/2AB, n=8 pairs. NS, not significant. In 100 µM glutamate experiments CNS4 alone pre-application evoked a transient and completely reversible current both with GluN1/2A and 1/2AB receptors and this was not observed with 0.3 µM glutamate experiments.

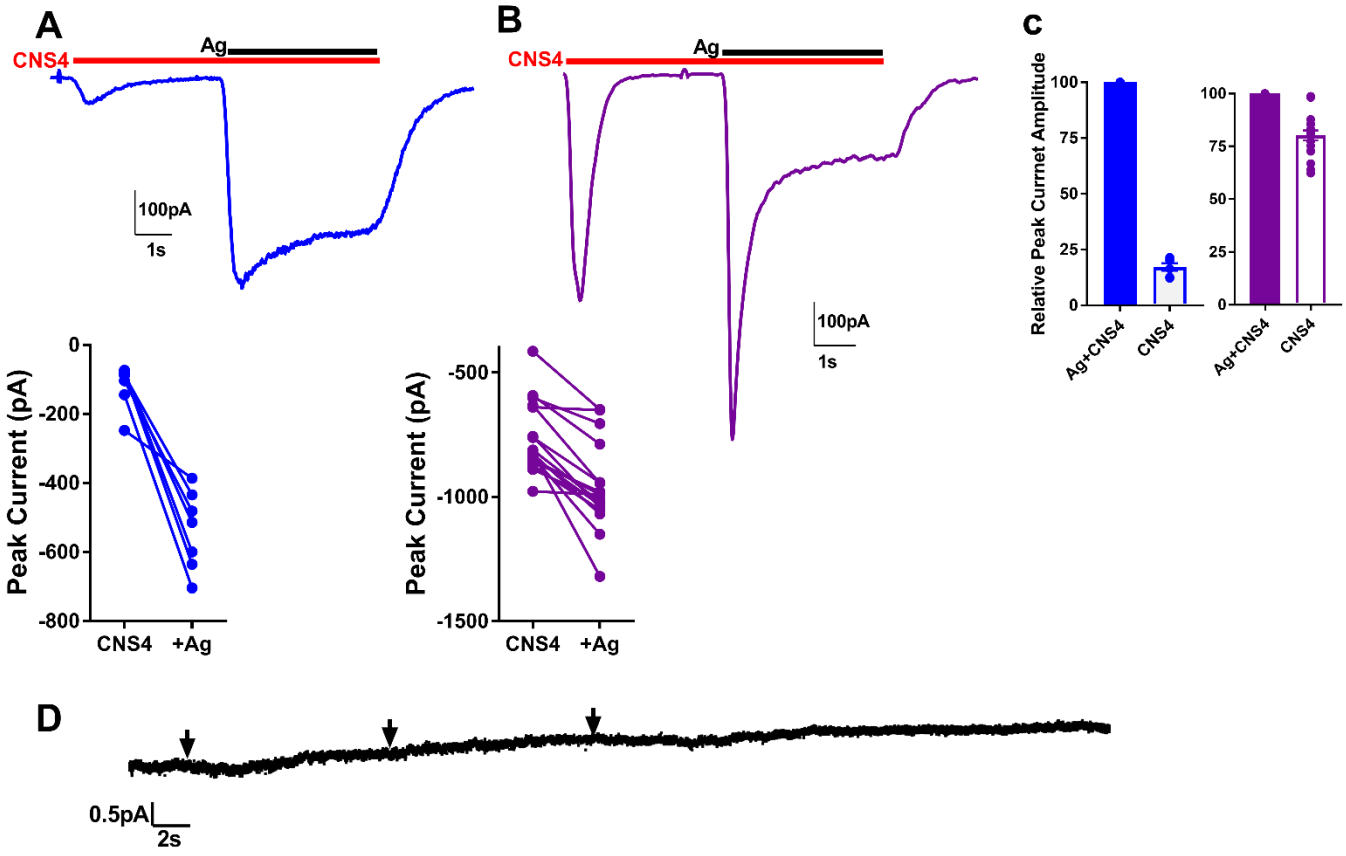

Figure 8. CNS4 sensitizes ambient glutamate in both GluN1/2A and 1/2B receptors. Traces represent whole cell patch-clamp current responses evoked by 100µM CNS4 (red) that was pre-applied before co-application with 100 µM glutamate and 100 µM glycine agonists (+Ag) in GluN1/2A (blue, **A**) and GluN1/2AB (purple, **B**) receptors. Peak current values of CNS4 and +Ag application were used for the analysis. Each pair of CNS4 alone and +AG application event is shown in dot plots. **C.** In the histograms, CNS4+Ag induced current response was normalized to hundred to calculate relative percentage current amplitudes. CNS4 alone application induced transient current was 17.24±1.6% (n=7) of CNS4+Ag current in GluN1/2A receptors. However in GluN1/2AB receptors this was as high as 80.15±2.3% (n=18) of maximal current amplitude. **D.** Trace shows similar whole cell patch clamp assay on an untransfected HEK293T cell, where CNS4 produced no current response. Arrowheads represent CNS4 application points.

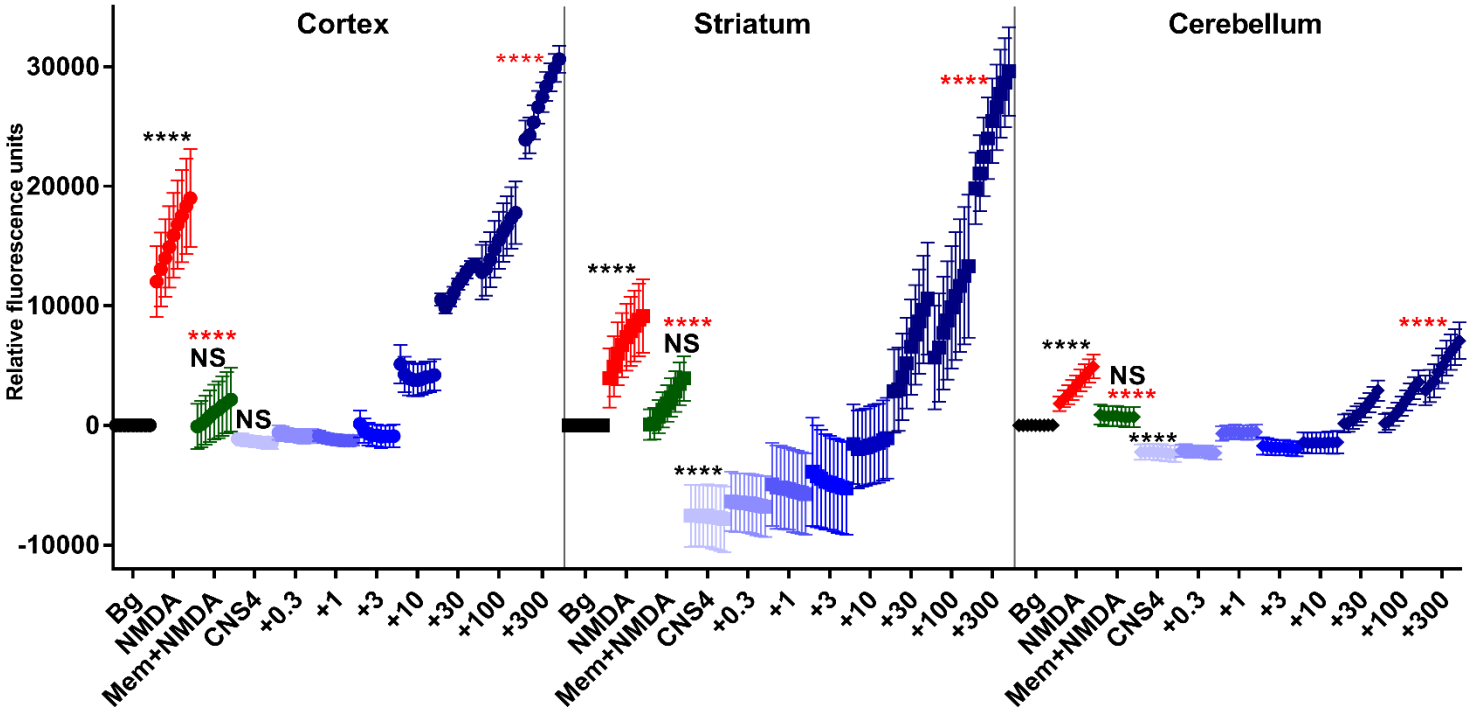

Figure 9. CNS4 potentiates Ca2+ ion influx in cultured rat brain cortical, striatal and cerebellar neurons. Dynamic calcium imaging assay was carried out using Fluo-8 no wash kit (abcam, ab112129). On DIV14 neurons were treated with the Fluo-8 dye and plates were incubated in 37C for 30min and in room temperature for 30min. Plates were then added with 100ul of volume of test chemicals (in HBSS) immediately before running the calcium flux assay by reading the fluorescence intensity at ex/em = 490/525nm using Synergy microplate reader, BioTek. Costar 96 well clear bottom black side plates were read from the bottom ten times with 60sec intervals between each read. Temperature was set at 37C and reading speed was 100mSec. First two columns (sixteen wells) served as background and their values were set to zero in the y-axis. Each treatment was applied on 8 wells, there were 10 treatments. In the treatment groups, each data point is an average (and SEM bars) background corrected values obtained from eight wells; each well was read ten times. Asterisk colors represent the comparison group. Bg, background; NMDA (red), 300uM NMDA; Mem+NMDA (green), 100uM NMDA + 50uM memantine; CNS4, 100uM CNS4. Increasing concentration of NMDA was added with 100uM CNS4, labeled as +0.3 to +300. (Light to dark blue). One-way ANOVA Tukey's multiple comparisons test was performed to identify the statistical significance between treatment groups. ****p<0.0001. Y-axis relative fluorescence units (rfu). NS= not significant.

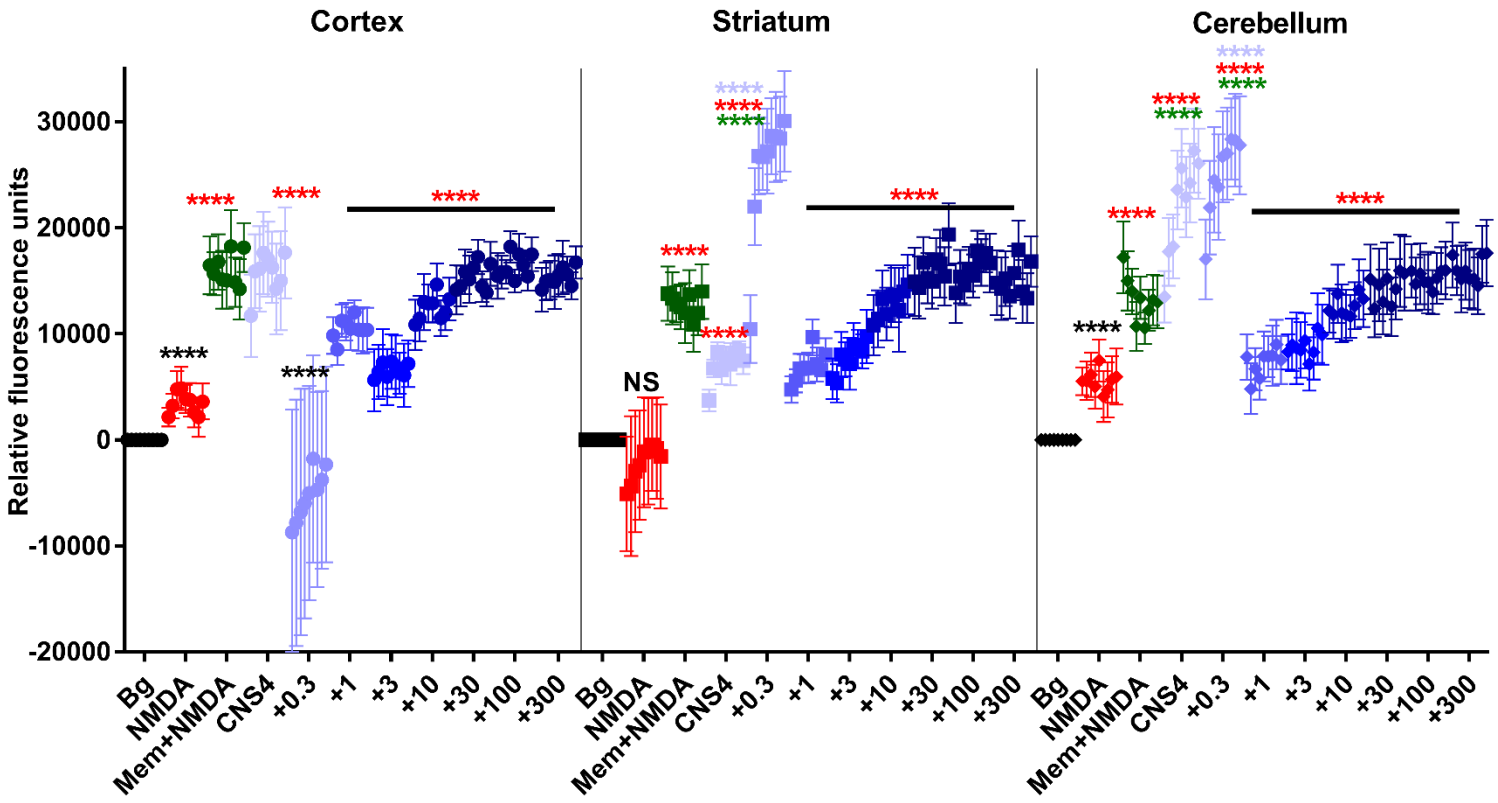

Figure 10. NMDA Concentration dependent potentiation of Na+ ions in cultured rat brain cortical, striatal and cerebellar neurons. Dynamic sodium imaging assay was carried out using CoroNa green-AM (ThermoFisher, cat # C36676), and the plate was read at 492/516nm using plate reader. On DIV14 neurons were treated with the dye and plates were incubated in 37C for 45min. Plates were washed then added with 100ul of volume of test chemicals (in HBSS) immediately before running the Na+ flux assay by reading the fluorescence intensity at ex/em = 492/516nM using Synergy microplate reader, BioTek. Costar 96 well clear bottom black side plates were read from the bottom ten times with 60sec intervals between each read. Temperature was set at 37C and reading speed was 100mSec. First two columns (sixteen wells) served as background and their values were set to zero in the y-axis. Each treatment was applied on 8 wells, there were 10 treatments. In the treatment groups, each data point is an average (and SEM bars) background corrected values obtained from eight wells; each well was read ten times. Asterisks colors represent the comparison group. Bg, background; NMDA (red), 300uM NMDA; Mem+NMDA (green), 100uM NMDA + 50uM memantine; CNS4, 100uM CNS4; Increasing concentration of NMDA was added with 100uM CNS4, labeled as +0.3 to +300. (Light to dark blue). One-way ANOVA Tukey's multiple comparisons test was performed to identify the statistical significance between treatment groups. ****p<0.0001. Y-axis relative fluorescence units (rfu). NS= not significant.

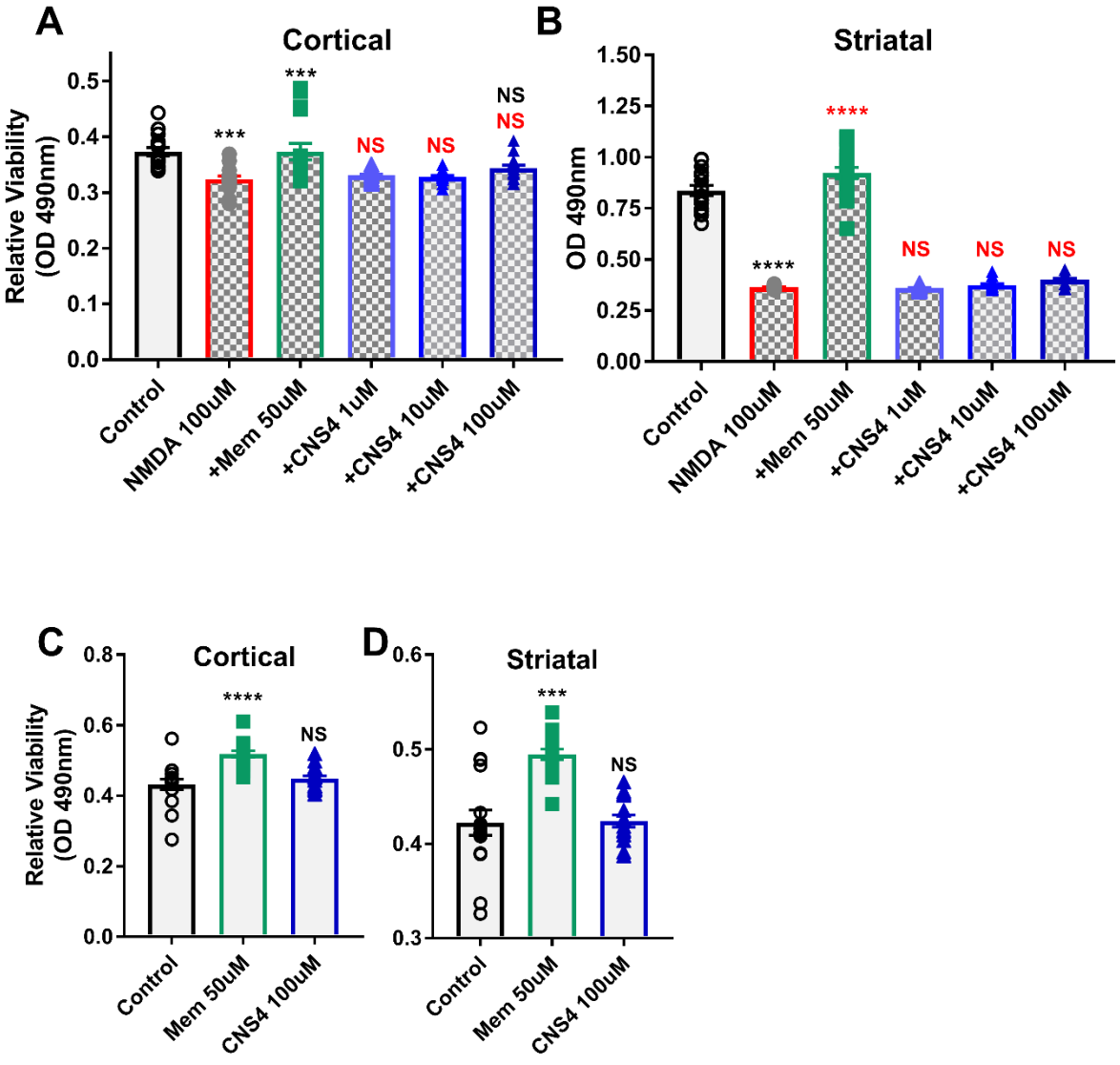

Figure 11. CNS4 induced potentiation of ion influx does not increase neurotoxicity. DIV14 rat brain cortical (**A&C**) or striatal (**B&D**) neurons were treated with vehicle (control) or other agents as labelled for overnight. MTS reagent was added and incubated for 2hrs before reading at 490nm using a microplate reader. Higher OD values in the y-axis represent better viability. Statistical significance was determined by One-way ANOVA Tuckey's multiple comparison test used to determine statistical significance of each treatment group with alpha level $p<0.05$. ***$p<0.001$, ****$p<0.0001$. A, B, C&D, n=16 wells for each control and treatment group. NS= not significant.

Extended Data Figure 1-1:

Synthesis of 4-fluoro-N-(2-(pyridin-3-yl)piperidine-1-carbonothioyl)benzamide (CNS004): Anabasine, piperidinylpyridine alkaloid, based a new thiourea was synthesized in two steps synthesis using thiocarbamoylation reaction. The starting 4-fluorobenzoyl isothiocyanate was synthesized *in situ* by heating 4-fluorobenzoyl chloride **1** with potassium thiocyanate in acetone. Further reaction of fluorobenzoyl isothiocyanate **2** with anabasine **3** in THF at room temperature yielded 4-fluoro-N-(2-(pyridin-3-yl)piperidine-1-carbonothioyl)benzamide (**CNS004**). The synthesized compound was confirmed by ^{1}H-NMR & LCMS analysis and HPLC purity >99%.

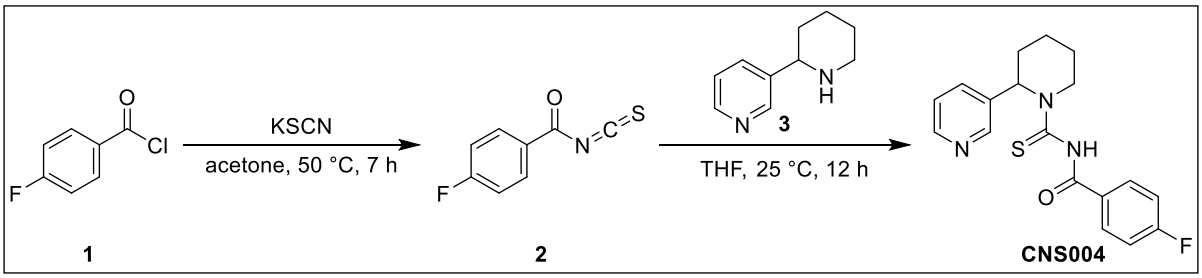

Experimental:

4-Fluorobenzoyl isothiocyanate (2): To a stirred solution of 4-fluoro benzoyl chloride **1** (2 g, 12.613 mmol) in dry acetone (15 mL) at room temperature under atmosphere was added potassium thiocyante (1.47 g, 15.136 mmol) at once. The reaction mixture was heated at 50 °C for 5 hours. After completion, the reaction mixture was filtered through a celite bed washed with acetone to remove inorganics. The filtrate was concentrated under *vacuo*. The obtained crude mixture was dissolved in a mixture of DCM/hexane (20 mL, 1:1 ratio) and passed through a pad of silica gel (230-400 mesh). The solvent was then evaporated under *vacuo* to get compound **2** gummy as a red colour solid, as such taken for the next step without further purification (Yield: 1.3 g).

4-Fluoro-N-(2-(pyridin-3-yl)piperidine-1-carbonothioyl)benzamide (CN004): To a stirred solution of anabasine **3** (0.1 g, 0.616 mmol) in dry THF (5 mL) at room temperature under nitrogen atmosphere was added compound **2** (0.11 g, 0.616 mmol) at once. The reaction mixture was stirred at room temperature for 16 hours. After completion, the reaction mixture was concentrated under *vacuo*. The crude mixture obtained was further purified by flash column chromatography on silica gel, 230-400 mesh using 20-25% of ethyl acetate in petroleum ether as an eluent to get **CNS004** as a pale-yellow solid (Yield: 0.13 g; 39% over two steps). ^{1}H-NMR (400 MHz, DMSO-d_6): δ 10.99 (br s, 1H), 8.72 (br s, 1H), 8.52 (d, J = 4.52 Hz, 1H), 8.08 (br s, 2H), 7.92 (br s, 1H), 7.46 (dd, J = 4.80, 7.92 Hz, 1H), 7.39-7.35 (m, 2H), 6.82 (br s, 1H), 4.02 (br s, 1H), 3.03 (dt, J =

5.16, Hz, 1H), 2.63-2.60 (m, 1H), 1.98 (br s, 1H), 1.65-1.62 (m, 3H), 1.42-1.40 (m, 1H); **LC_MS:** Calc. for $C_{18}H_{18}FN_3OS$, 343.42; Obs. 344.2 $[M+H]^+$.

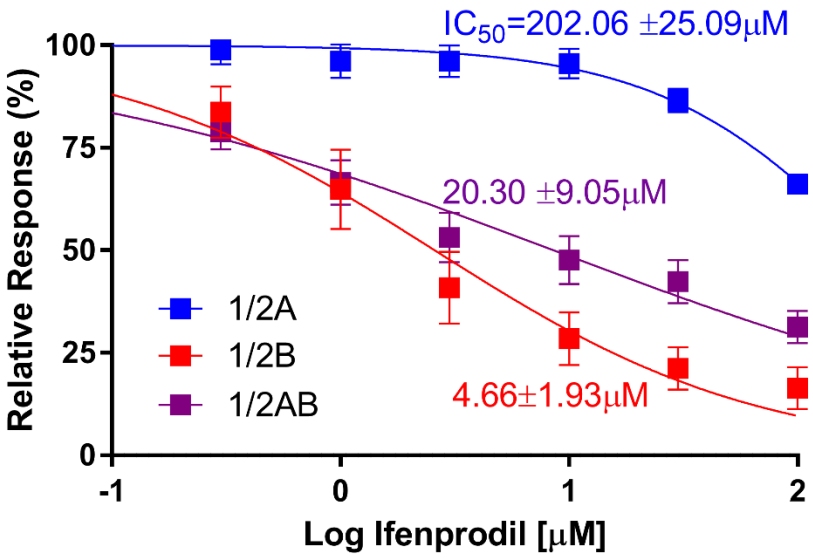

Extended Data Figure 1-2:

Ifenprodil inhibits GluN1/2AB receptors with an IC50 that is intermediate to GluN1/2A and 1/2B receptors. Ifenprodil dose response curve was performed in the presence of 100µM glutamate and 100uM glycine concentration. GluN1/2A (n=5), 1/2B (n=6) & 1/2AB (n=8). IC50 values obtained by a non-linear fit are provided in the figure.

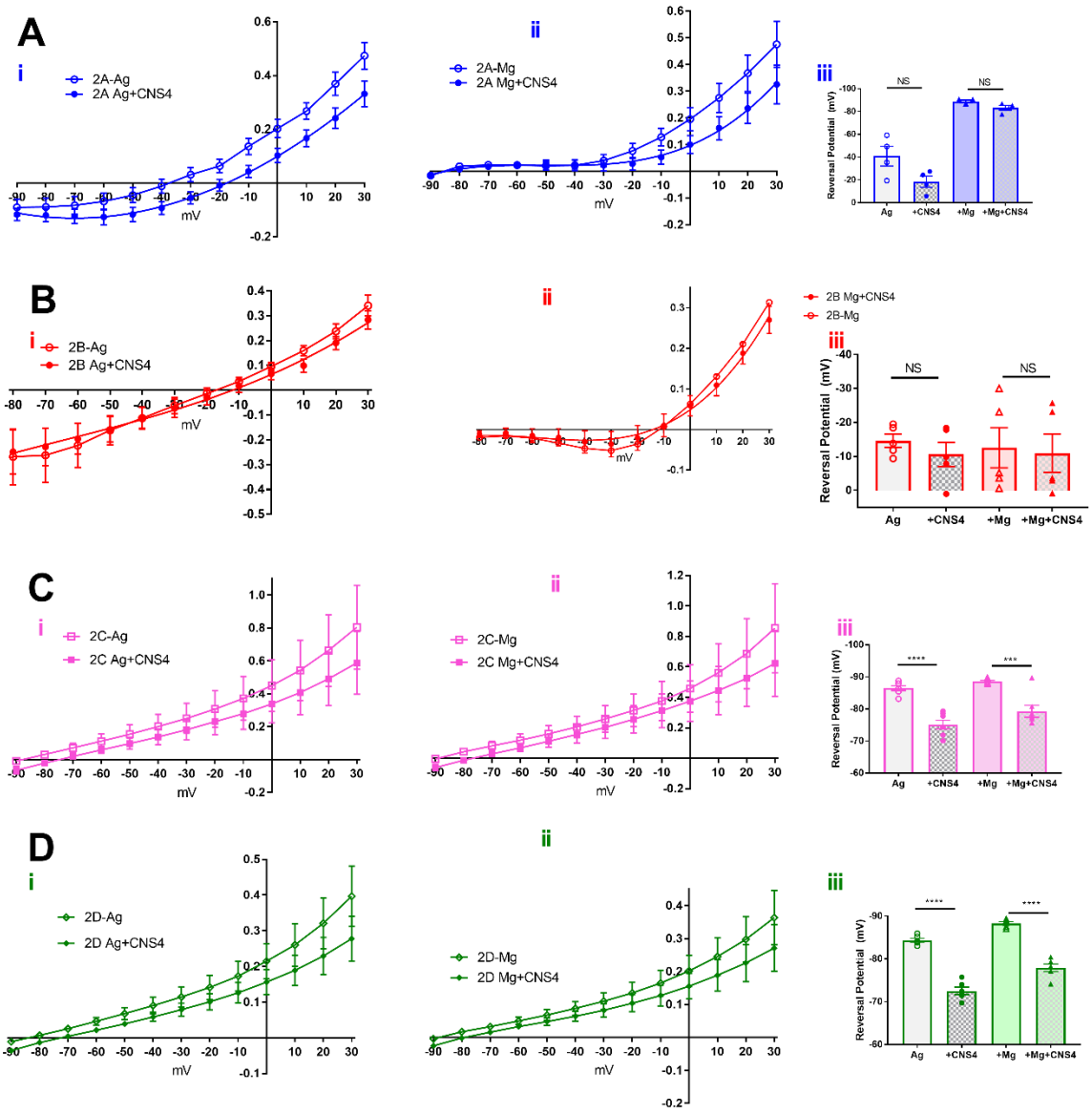

Extended Data Figure 4-1. Voltage independent activity of CNS4. 100uM glycine and 100uM glutamate was used as agonist to activate the receptors. Agonist induced whole cell current-voltage (I-V) relationship was studied in 10mV intervals ranging from -90mv to +30mv. Recording buffer contained 116 mM NaCl, 2 mM KCl, 0.3 mM BaCl2, and 5 mM HEPES, pH 7.4. I-V relationship of 100uM CNS4 on agonist induced currents in the presence and absence of 40uM MgCl2 was studied. 40uM MgCl2 was chosen from the previously published experiments (Bledsoe et al, 2019), since this was the IC50 (at -60mV) of GluN1/2A receptors. Data points were

aligned by least square fit by third order polynomial equation, (Y=B0 + B1*X +B2*X^2 + B3*X^3), except for GluN1/2B that needed a fourth order polynomial equation. Reversal potential was obtained (from x-axis values when y=0.) for each individual recordings and then averaged. In GluN1/2C receptors, CNS4 altered 0.3uM glutamate (**A,B,C,&D**) induced inward current reversal potential in the absence (-86.44± 0.74 vs -75.15±1.33 mv, p<0.0001, n=7) and presence (-88.59± 0.30 vs -79.25±1.87mv, p<0.001, n=7) of Mg2+. A similar reduction was observed with GluN1/2D receptors, (-84.35± 0.42mv vs -72.52±0.85mv, p<0.0001, n=6) and presence (-88.29± 0.35mv vs -77.88±0.87mv, p<0.0001, n=6) of Mg2+. Statistics, One-Way ANOVA with Tukey's multiple comparisons test, alpha level <0.05. Current values are obtained from the last one second of the 5 second application.

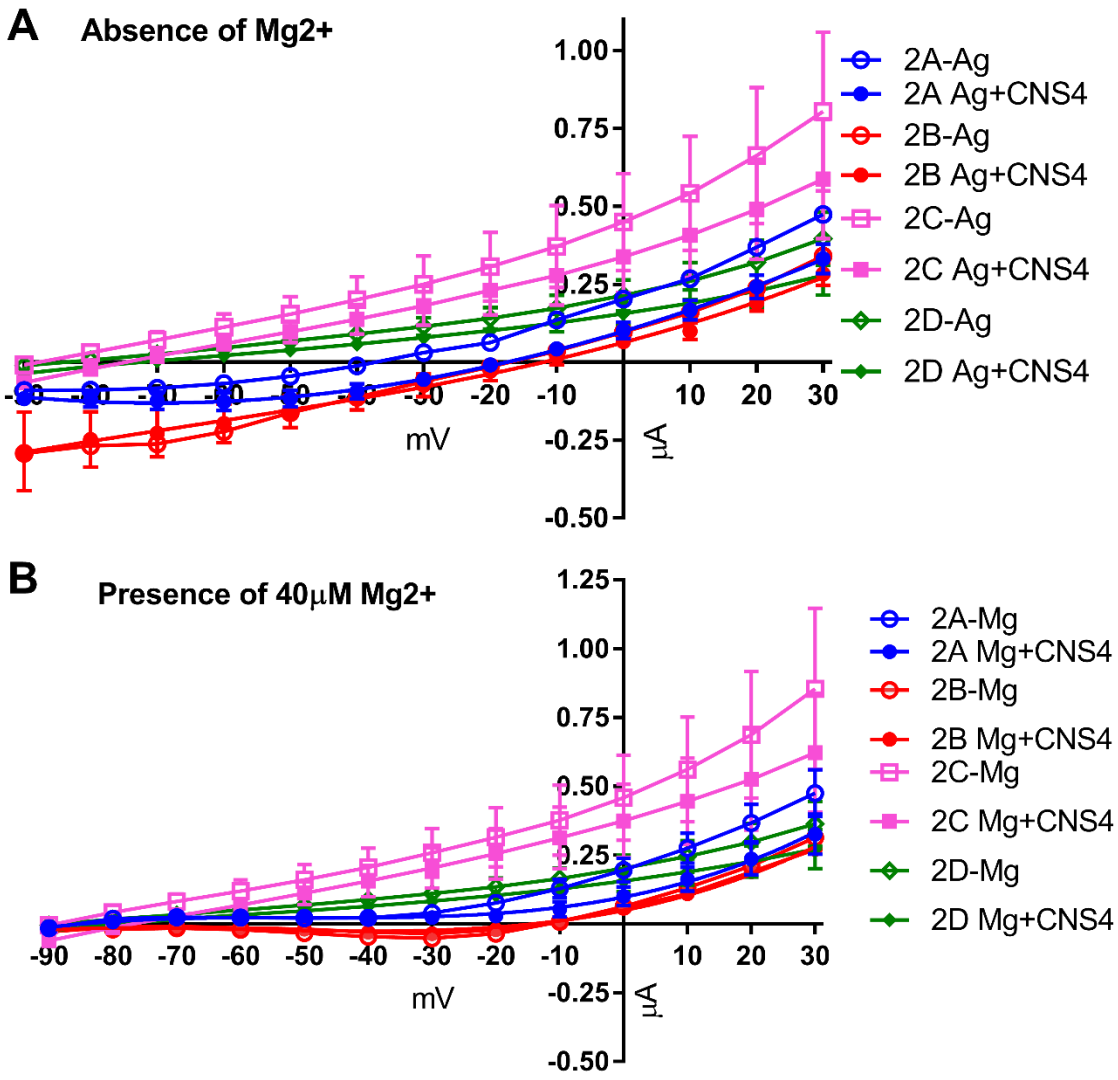

Extended Data Figure 4-2: Voltage independent activity of CNS4 at low glutamate concentration. 0.3uM glutamate and 100uM glycine was used as agonist to activate the receptors. Agonist induced whole cell current-voltage (I-V) relationship was studied in 10mV intervals ranging from -90mv to +30mv. Recording buffer contained 116 mM NaCl, 2 mM KCl, 0.3 mM BaCl2, and 5 mM HEPES, pH 7.4. I-V relationship of 100uM CNS4 on agonist induced currents in the absence (**A**) and presence (**B**) of 40uM MgCl2 was studied. Data points were

aligned by least square fit by third order polynomial equation, (Y=B0 + B1*X +B2*X^2 + B3*X^3), except for GluN1/2B that needed a fourth order polynomial equation. Reversal potential was obtained (from x-axis values when y=0.) for each individual recordings and then averaged.

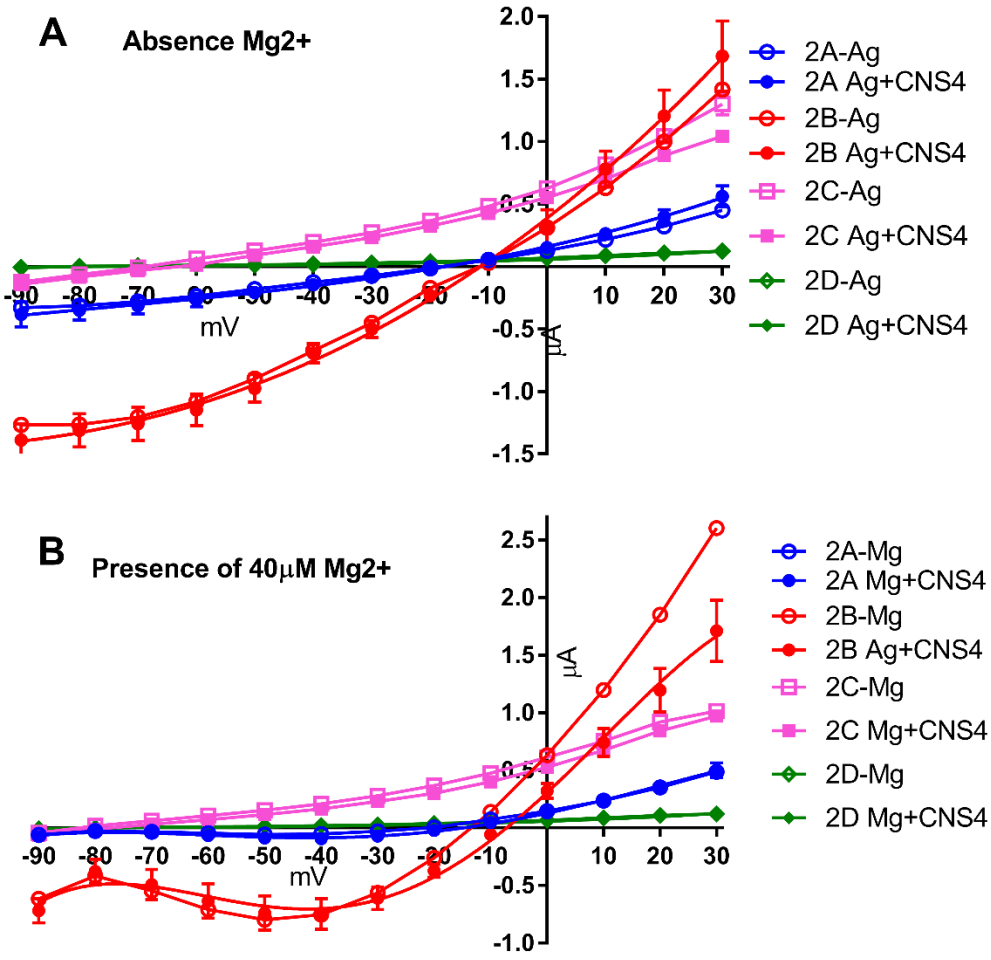

Extended Data Figure 4-3: Voltage independent activity of CNS4 at high glutamate concentration. 100uM glycine and 100uM glutamate was used as agonist to activate the receptors. Agonist induced whole cell current-voltage (I-V) relationship was studied in 10mV intervals ranging from -90mv to +30mv. Recording buffer contained 116 mM NaCl, 2 mM KCl, 0.3mM BaCl2, and 5mM HEPES, pH 7.4. I-V relationship of 100uM CNS4 on agonist induced currents in the absence (**A**) and presence (**B**) of 40uM MgCl2 was studied. Data points were aligned by least square fit by third order polynomial equation, (Y=B0 + B1*X +B2*X^2 + B3*X^3), except for GluN1/2B that needed a fourth order polynomial equation. Reversal potential was obtained (from x-axis values when y=0.) for each individual recordings and then averaged.

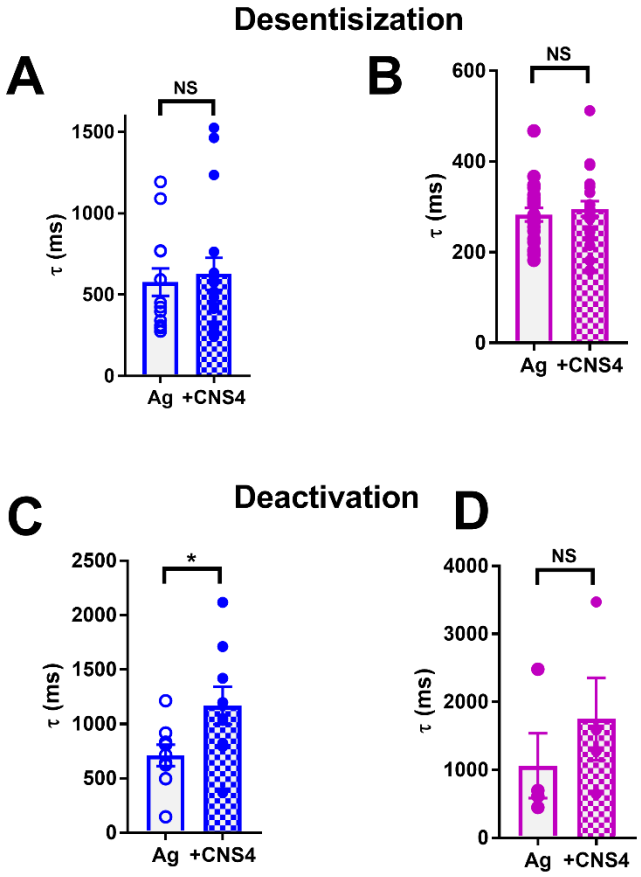

Extended Data Figure 5-1: Effect of CNS4 on desensitization and deactivation of GluN1/2A and 1/2AB receptors. Traces obtained from the whole cell patch-clamp electrophysiology assays, were analyzed for CNS4 induced desensitization (A&B) and deactivation (C&D) time constants (tau) in GluN1/2A (blue) and GluN1/2AB (purple) receptors. Decay time constant (tau) was calculated using exponential weighted fit component of clampfit 10.7 (pClamp) software. Unpaired –t- test, *p<0.05. NS, not significant. GluN1/2A deactivation time course was significantly increased (Ag, 710.9 ± 98.27ms, n=9 vs Ag+CNS4, 1067 ± 104.3ms, n=19, p<0.05, unpaired t-test) after CNS4 co-application. This reveals a slower dissociation of agonists from the GluN1/2A receptor. Ag= 100uM glutamate and glycine. +CNS = Ag+CNS4.

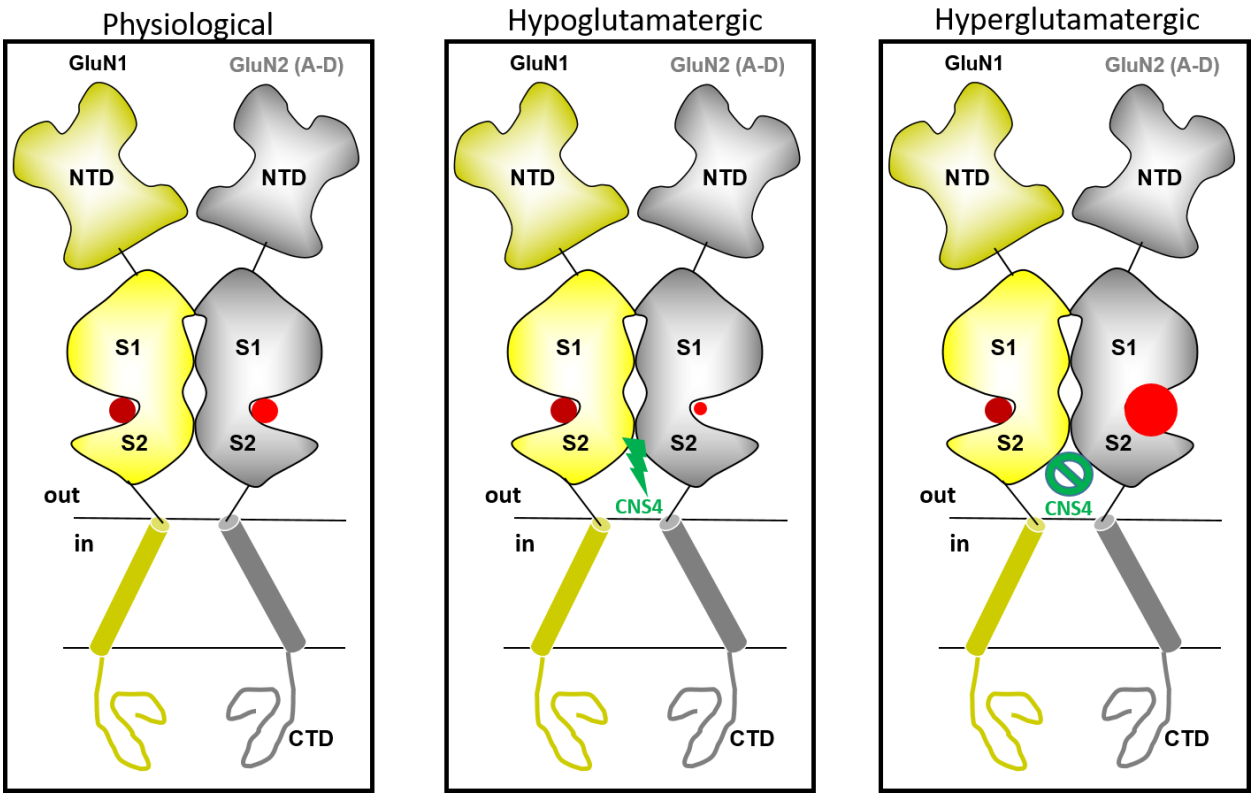

Graphical figure: Schematic diagrams represent topology of NMDA receptors domains. For clarity only two subunits (GluN1 & GluN2) are presented. NTD, N-terminal domain, S1&S2 are segments forming agonist binding domain. Tubes represent channel forming transmembrane domains. CTD, C-terminal domain. In and out, intra and extracellular side. Maroon circle, glycine. Size of red circle represent normal, hypo- and hyper- glutamatergic conditions. CNS4 potentiates NMDA receptors when there was low glutamate, and inhibits the receptors when high glutamate was present. Thus, CNS4 acts like a NMDA receptor optimizer.